

1967

An analog simulation of the Chezem-Helmick model of a two-core reactor

Alberto Manuel Campos
Iowa State University

Follow this and additional works at: <https://lib.dr.iastate.edu/rtd>

 Part of the [Nuclear Engineering Commons](#), and the [Oil, Gas, and Energy Commons](#)

Recommended Citation

Campos, Alberto Manuel, "An analog simulation of the Chezem-Helmick model of a two-core reactor " (1967). *Retrospective Theses and Dissertations*. 3996.
<https://lib.dr.iastate.edu/rtd/3996>

This Dissertation is brought to you for free and open access by the Iowa State University Capstones, Theses and Dissertations at Iowa State University Digital Repository. It has been accepted for inclusion in Retrospective Theses and Dissertations by an authorized administrator of Iowa State University Digital Repository. For more information, please contact digirep@iastate.edu.

This dissertation has been
microfilmed exactly as received 68-2804

CAMPOS, Alberto Manuel, 1921-
AN ANALOG SIMULATION OF THE CHEZEM-HELMICK
MODEL OF A TWO-CORE REACTOR.

Iowa State University, Ph.D., 1967
Engineering, nuclear

University Microfilms, Inc., Ann Arbor, Michigan

AN ANALOG SIMULATION OF THE CHEZEM-HELMICK
MODEL OF A TWO-CORE REACTOR

by

Alberto Manuel Campos

A Dissertation Submitted to the
Graduate Faculty in Partial Fulfillment of
The Requirements for the Degree of
DOCTOR OF PHILOSOPHY

Major Subject: Nuclear Engineering

Approved:

Signature was redacted for privacy.

In Charge of Major Work

Signature was redacted for privacy.

Head of Major Department

Signature was redacted for privacy.

Dean of Graduate College

Iowa State University
Of Science and Technology
Ames, Iowa

1967

TABLE OF CONTENTS

	Page
INTRODUCTION	1
Survey of Earlier Work	2
THE CHEZEM-HELMICK MODEL OF A TWO-CORE REACTOR	4
Kinetic Equations of the Pulsed Coupled System	4
Results of the Chezem-Helmick Experiment	12
AN ANALOG SIMULATION OF THE CHEZEM-HELMICK TWO-CORE MODEL	19
Transformation of the Equations	20
Initial Conditions	22
Analog Solutions	26
Problem Set-Up and Scaling	28
Discussion of Results	37
AN APPLICATION OF THE ANALOG SIMULATOR	39
Effect of Reactivity Drops on Neutron Generation Rates	39
Solution of the Exact Differential Equations (Four Roots)	59
Solution of the Exact Differential Equations (Two Roots)	63
Effect of the Coefficients K_1	66
Summary of Results	68
CONCLUSIONS AND RECOMMENDATIONS FOR FURTHER STUDY	86
LITERATURE CITED	88
APPENDIX A	90
Computation of the K 's	90

	Page
APPENDIX B	93
Expansion and Evaluation of ΣW_i , $\Sigma R_i W_i$, $\Sigma R_i^2 W_i$, $\Sigma R_i^3 W_i$	93
APPENDIX C	96
Sample Computation for the Four-Root Case	96
APPENDIX D	99
Sample Computation for the Two-Root Case	99

INTRODUCTION

During the last few years research in the kinetics of coupled-core reactors has greatly increased. Multimodule or multicore designs, possessing strong coupling effects, have been suggested, as in propulsion reactors of the Rover Nuclear Rocket Program. The reason for the interest in this type of reactors is its economics and the possibility of increased safety and reliability. However, the question of the stability and control of such reactors is not readily resolved, hence the need of some form of simulation of these reactors for more careful analysis of them prior to their actual construction.

This work is a study of the possibility of constructing one such analog, specifically for the Chezem-Helmick model of the two-core reactor. This model was chosen because of its simplicity and its adequacy to predict kinetic behavior in cases where the cores are not too strongly coupled. An analog simulator is here constructed and tested against the experimental data on which Chezem and Helmick based their model, and an analysis is then made of sixteen related cases to show one use of the analog.

It is hoped that this work will afford some modest contribution to the preliminary analysis of two-core reactor systems and suggest ways of making the analog simulator a useful tool in teaching and research.

Survey of Earlier Work

A general theory of coupled core reactors was introduced by Avery in 1958; existing formulations range from those of Cockrell, of Hansen and of Gage, based on transport theory, to the one-velocity diffusion treatment by Baldwin. S. J. Gage (6) gives a comprehensive survey of the many theories, sometimes branching and interrelated, which culminates in a unified approach to the problems of spatial and spectral coupling in reactor kinetics. His unified theory is then applied and tested on various two-core models, one of them being that of Chezem and Helmick.

A few years ago, spurred by the interest in nuclear rocket propulsion for space age needs, the Los Alamos Scientific Laboratory started a series of research projects on multiple-core reactors. A simple theory, subsequently verified by experiment, was given by Chezem and Helmick mainly in Reference (4) and also treated in the other papers by either author and by Seale. See References (4), (5), (11), (12) and (13).

Work on electronic analog computing with applications to reactor kinetics has been done extensively at Argonne National Laboratories by the group headed by G. S. Pawlicki. Bryant et al. (2) published a basic treatment of electronic analog computing with sample applications, a few of which are in nuclear reactor kinetics. Analog studies in reactor kinetics

have been made by Hang and Manning (7) for the single core reactor taking into consideration six groups of delayed neutrons.

This thesis is a start in the preparation of an analog that will be for two-core reactors what the Hang and Manning work is for single-core reactors; it is only a start--some improvement and refinement of technique and instrumentation must be done before the method can be considered as satisfactory.

THE CHEZEM-HELMICK MODEL OF A TWO-CORE REACTOR

In September and October, 1964 the Los Alamos Coupled Reactor Experiment was performed with two Kiwi-type reactors operating in proximity. As a part of the program one of the reactors was excited by 3-microsecond pulses of 14-Mev neutrons from a pulse generator. The neutron generation rates in the pulsed core and in the passive core were followed by time-delay analyzers operating from neutron detectors located at the centers of the cores. The driving core, designated as Core No. 1, was the Pajarito Research Kiwi Assembly (PARKA) reactor and the passive core, Core No. 2, was the Kiwi-TNT reactor assembly subsequently destroyed in January 1965 in a test at the Nuclear Reactor Development Station in Nevada.

C. G. Chezem and H. H. Helmick (4) developed kinetic equations of the pulsed coupled system, and the response functions obtained from the experiment were in good agreement with the prediction of their theory. This section will be devoted to a brief exposition of the Chezem-Helmick formulation and of the calculations and experimental results obtained.

Kinetic Equations of the Pulsed Coupled System

The Chezem-Helmick approach to the kinetics problem of coupled-core reactors is basically a simplification of the formulations by Hansen (8) and by Seale (12) of the Baldwin method. The simplification consists in adopting the

"two-point" reactor kinetics equation, in assuming "lumped parameters" and in ignoring delayed neutrons.

A "two-point" kinetics equation assumes that space is divided into two "points," one corresponding to the reactor proper and the other to the environment. It is assumed that one set of parameters suffices to characterize each "point;" this is essentially what is implied in the term "lumped parameters." A cluster of reactors can be described by "two-point" kinetics equations by considering each reactor in turn as the reactor proper and the others as part of the "environment" with respect to it. There will be, therefore, source terms corresponding to each of the other reactors in the cluster. For an n-cluster arrangement, this gives rise to n "two-point" kinetics equations if the reactors are nearly critical.

According to this simplified version of the theory, the general equation for the neutron generation rate¹ at the i-th core, G_i , of a coupled array of m cores, neglecting delayed neutrons, is

$$\frac{dG_i(t)}{dt} = \frac{\delta k_i^P}{l_i^*} G_i(t) + \frac{1}{l_i^*} \sum_{\substack{j=1 \\ j \neq i}}^m \epsilon_{ij} \int_0^t G_j(t-T) P(T) dT + A \delta_{i1} \delta(t) \quad (1)$$

¹The neutron generation rate, G_i , here corresponds to the "effective prompt neutron production rate" in Hansen (8) and is defined by the equation $G_i = N_i/l_i$, where N_i is the "effective" neutron population in the reactor and l_i is the prompt neutron lifetime. The units of G_i are then $\bar{n}/\text{cm}^3\text{-sec}$.

where $\epsilon_{ij} G_j(t-T) P(T)$ is the effective source strength for core i at time t contributed by fissions in core j at time T earlier, and its integral over T is the combined effect of all such sources from the start, at $T = 0$, to $T = t$, the instant under consideration. The quantity $P(T)$ is a probability factor and under the normalization $\int P(T) dT = 1$, ϵ_{ij} becomes the neutron effectiveness for core i of fission neutrons born in the j -th core, and depends on the geometry of the system. $P(T)$ is chosen, assuming the fissions as random unrelated events, to be

$$P(T) = \frac{1}{\tau_{ij}} e^{-\frac{T}{\tau_{ij}}} \quad (2)$$

where τ_{ij} is an interaction time of neutrons between the j -th and i -th cores. This interaction time can be related to the separation between the point reactor sources and the leakage flux and its adjoint.

Other quantities involved in Equation 1 are defined as follows: λ_i^* is the neutron lifetime, expressed in units of β , i.e., $\lambda_i^* = \frac{\lambda_i}{\beta}$. The term δk_i^P is the excess prompt reactivity of the i -th core when isolated from its environment. The source term $A \delta_{i1} \delta(t)$ represents a "delta-function type" pulse of neutrons in Core No. 1 at $t = 0$.

It is more convenient to work with the Laplace transform of Equation 1 than with the equation as written. With $P(T)$ given by Equation 2 and the usual assumption of zero initial condition, this is

$$sg_i(s) = \frac{\delta k_i^P}{l_i^*} g_i(s) + \frac{1}{l_i^*} \sum_{\substack{j=1 \\ j \neq i}}^m \frac{\epsilon_{ij}}{\tau_{ij}} \frac{1}{s + \frac{1}{\tau_{ij}}} g_j(s) + A\delta_{il}$$

or

$$sg_i(s) = \alpha_i g_i(s) + \sum_{\substack{j=1 \\ j \neq i}}^m \gamma_{ij} \frac{1}{s + \frac{1}{\tau_{ij}}} g_j(s) + A\delta_{il} \quad (3)$$

where $\alpha_i = \frac{\delta k_i^P}{l_i^*}$ and $\gamma_{ij} = \frac{\epsilon_{ij}}{l_i^* \tau_{ij}}$.

For a system consisting of only two cores, assume $l_1 = l_2 = l$, $\epsilon_{12} = \epsilon_{21} = \epsilon$ and $\tau_{12} = \tau_{21} = \tau$, so Equation 3 becomes these two equations:

$$\left. \begin{aligned} sg_1(s) &= \alpha_1 g_1(s) + \frac{\gamma}{s + \frac{1}{\tau}} g_2(s) + A \\ sg_2(s) &= \alpha_2 g_2(s) + \frac{\gamma}{s + \frac{1}{\tau}} g_1(s) \end{aligned} \right\} \quad (4)$$

$$\left. \begin{aligned} \text{or } (s-\alpha_1)g_1(s) - \frac{\gamma}{s + \frac{1}{\tau}} g_2(s) &= A \\ -\frac{\gamma}{s + \frac{1}{\tau}} g_1(s) + (s-\alpha_2)g_2(s) &= 0 \end{aligned} \right\} \quad (5)$$

These are simultaneous equations in $g_1(s)$ and $g_2(s)$ and can be solved. The determinant of the coefficients of $g_1(s)$ and $g_2(s)$ is

$$D = \begin{vmatrix} s-\alpha_1 & -\frac{\gamma}{s + \frac{1}{\tau}} \\ -\frac{\gamma}{s + \frac{1}{\tau}} & s-\alpha_2 \end{vmatrix} = (s-\alpha_1)(s-\alpha_2) - \frac{\gamma^2}{(s + \frac{1}{\tau})^2},$$

$$\text{or } D = \frac{(s-\alpha_1)(s-\alpha_2)(s+\frac{1}{\tau})^2 - \gamma^2}{(s+\frac{1}{\tau})^2}, \quad (6)$$

and the solutions for $g_1(s)$ and $g_2(s)$ are

$$g_1(s) = \frac{\begin{vmatrix} A & -\frac{\gamma}{s+\frac{1}{\tau}} \\ 0 & s-\alpha_2 \end{vmatrix}}{D} = \frac{A(s-\alpha_2)}{D}$$

$$\text{or } \frac{g_1(s)}{A} = \frac{(s-\alpha_2)(s+\frac{1}{\tau})^2}{(s-\alpha_1)(s-\alpha_2)(s+\frac{1}{\tau})^2 - \gamma^2}, \quad (7)$$

$$\text{and } g_2(s) = \frac{\begin{vmatrix} s-\alpha_1 & A \\ -\frac{\gamma}{s+\frac{1}{\tau}} & 0 \end{vmatrix}}{D} = \frac{A \frac{\gamma}{s+\frac{1}{\tau}}}{D}$$

$$\text{or } \frac{g_2(s)}{A} = \frac{\gamma(s+\frac{1}{\tau})}{(s-\alpha_1)(s-\alpha_2)(s+\frac{1}{\tau})^2 - \gamma^2}. \quad (8)$$

If the denominator of Equations 7 and 8 can be expressed in factored form thus

$$(s-\alpha_1)(s-\alpha_2)(s+\frac{1}{\tau})^2 - \gamma^2 = \prod_{i=1}^4 (s-R_i) \quad (9)$$

then, by the method of inverse Laplace transforms the following equations are obtained for the neutron generation rates $G_1(t)$ and $G_2(t)$:

$$\frac{G_1(t)}{A} = \sum_{i=1}^4 \frac{(R_i - \alpha_2) \left(R_i + \frac{1}{T}\right)^2}{4 \prod_{\substack{j=1 \\ j \neq i}}^4 (R_i - R_j)} e^{R_i t}$$

$$\text{or } \frac{G_1(t)}{A} = \sum_{i=1}^4 U_i e^{R_i t} \quad \text{where } U_i = \frac{(R_i - \alpha_2) \left(R_i + \frac{1}{T}\right)^2}{4 \prod_{\substack{j=1 \\ j \neq i}}^4 (R_i - R_j)}, \quad (10)$$

$$\text{and } \frac{G_2(t)}{A} = \sum_{i=1}^4 \frac{\gamma \left(R_i + \frac{1}{T}\right)}{4 \prod_{\substack{j=1 \\ j \neq i}}^4 (R_i - R_j)}$$

$$\text{or } G_2(t) = \sum_{i=1}^4 V_i e^{R_i t} \quad \text{where } V_i = \frac{\gamma \left(R_i + \frac{1}{T}\right)}{4 \prod_{\substack{j=1 \\ j \neq i}}^4 (R_i - R_j)}. \quad (11)$$

To find the roots R_i of the denominators of Equations 7 and 8 use is made of the Raphson modification of the Newton method of approximation. As a first approximation to the roots use is made of whichever of the Equations 12 through 17 may apply.

$$\text{If } \alpha_1 \neq \alpha_2, R_1 = \alpha_1 + \frac{\gamma^2}{(\alpha_1 - \alpha_2) \left(\alpha_1 + \frac{1}{T}\right)^2} \quad (12)$$

$$\text{and } R_2 = \alpha_2 - \frac{\gamma^2}{(\alpha_1 - \alpha_2) \left(\alpha_2 + \frac{1}{T}\right)^2}. \quad (13)$$

$$\text{If } \alpha_1 = \alpha_2 = \alpha, R_{1,2} = \alpha \pm \frac{\gamma}{\alpha + \frac{1}{\tau}}. \quad (14)$$

$$\text{If } \tau_{12} = \tau_{21} = \tau, R_{3,4} = -\frac{1}{\tau} \pm \sqrt{\frac{\gamma^2}{(\alpha_1 + \frac{1}{\tau})(\alpha_2 + \frac{1}{\tau})}}. \quad (15)$$

$$\text{If } \tau_{12} \neq \tau_{21}, R_3 = -\frac{1}{\tau_{12}} + \frac{\gamma_{12} \gamma_{21}}{(\alpha_1 + \frac{1}{\tau_{12}})(\alpha_2 + \frac{1}{\tau_{21}})(\frac{1}{\tau_{21}} - \frac{1}{\tau_{12}})} \quad (16)$$

$$R_4 = -\frac{1}{\tau_{21}} - \frac{\gamma_{12} \gamma_{21}}{(\alpha_1 + \frac{1}{\tau_{21}})(\alpha_2 + \frac{1}{\tau_{12}})(\frac{1}{\tau_{21}} - \frac{1}{\tau_{12}})} \quad (17)$$

From the assumptions of the theory it seems to follow that all the roots R_i are negative real numbers that increase numerically as one goes from R_1 to R_4 . The roots R_i are seen from the above equations to fall into two groups: R_1 and R_2 depend on α_i , and are called the Rossi- α -dominated roots; and R_3 and R_4 depend very much on τ and are called the τ -dominated roots. The cases treated here are those where the α 's are relatively small, so the Rossi- α dominated roots are numerically much less than the τ -dominated roots. The latter pair give rise to fast-decaying exponential functions and become negligible after a few milliseconds.

Chezem and Helmick used a computer program (PULS) to solve Equations 10 and 11 for $G_1(t)$ and $G_2(t)$. All parameters of the calculations were determined experimentally, except τ , the time-lag, which was approximated by

$$\tau = x \frac{\sum_g \mathcal{L}_g \mathcal{L}_g^+ / v_g}{\sum_g \mathcal{L}_g \mathcal{L}_g^+} \quad (18)$$

where \mathcal{L}_g is the calculated leakage flux by energy group g and \mathcal{L}_g^+ is the leakage adjoint flux from a Kiwi-B core. The quantity x represents the center-to-center spacing of the cores, and v_g is the average velocity of neutrons in the g -th energy group.

Parameters common to both cores are, from Chezem and Helmick (4),

$$\beta = 0.0078$$

$$l_1 = l_2 = l = 31 \text{ } \mu\text{sec}$$

$$\epsilon_{12} = \epsilon_{21} = \epsilon = \begin{cases} 0.306 \text{ } \$ \text{ (at 6 ft)} \\ 0.169 \text{ } \$ \text{ (at 9 ft)} \end{cases}$$

$$\tau_{12} = \tau_{21} = \tau = \begin{cases} 130 \text{ } \mu\text{sec (at 6 ft)} \\ 190 \text{ } \mu\text{sec (at 9 ft)} \end{cases}$$

The measured coupling coefficient ϵ includes the effect of room return and is not the free-space coupling coefficient.

The time t_p of the peak of the response curve of Core No. 2 can be approximated readily. If $\alpha_1 \approx \alpha_2 \approx \alpha$ the two roots R_1 and R_2 will differ from α by a slight amount, and can therefore be approximated as $(\alpha + \Delta\alpha)$ and $(\alpha - \Delta\alpha)$ respectively. Hence

$$G_2(t) \sim e^{(\alpha + \Delta\alpha)t} - e^{(\alpha - \Delta\alpha)t}$$

which for small $\Delta\alpha$ (loose coupling) can be written as

$$G_2(t) \sim 2\Delta\alpha t e^{\alpha t}.$$

This function has a maximum at $t = t_p$ where $t_p = -\frac{1}{\alpha}$, and if α_1 is nearly equal to α_2 , α may be taken as the average:

$$\alpha = \bar{\alpha} = \frac{\alpha_1 + \alpha_2}{2}.$$

Results of the Chezem-Helmick Experiment

Four cases were considered, corresponding to different actual core separations and reactivity settings. These conditions with computed and observed parameters are shown in Table 1 and composite results are shown in Figures 1 through 4.

A Roman numeral is used to designate each case, shown in Column (1) of Table 1. Column (2) gives the core separation in feet, and Columns (3) and (4) list the reactivity settings of the two cores and the computed Rossi- α values. The parameter A is chosen to agree with the $t=0$ intercept in the least-squares fitting for a series of exponential functions to the experimental points, done by computer, and Column (5) gives the value of A determined in this way.¹ Column (6) shows the calculated values of the roots R_1 , and Columns (7) and (8) give the coefficients of the exponential terms corresponding

¹The values of A for Cases II and III shown in Column (4) of Chezem and Helmick's Table I (4, page 12) are in error by a factor of 10. They should be 8.85×10^7 and 7.71×10^7 , respectively, to conform to the values given in Columns (5) and (6) of the same table.

Table 1. Comparison of theory and results of pulsed coupled core experiment^a

(1) Case	(2) Separation x (ft)	(3) δk_1^P (\$) and α_1	(4) δk_2^P (\$) and α_2	(5) A	(6) R_i	(7) U_i	(8) V_i	(9) $t_P = \frac{1}{\alpha}$
I	6	-2.200 -553.5	-2.060 -518.3	3.63×10^8	-452	+0.3883	+0.4813	0.0019
					-622	+0.6119	-0.4929	
					-7609 -7774	-0.005921 +0.005646	+0.005958 +0.005621	
II	6	-1.630 -410.1	-1.527 -384.2	8.85×10^7	-316	+0.4147	+0.4897	0.0025
					-480	+0.5855	-0.5009	
					-7610 -7773	-0.005732 +0.005469	+0.005729 +0.005412	
III	9	-1.609 -404.8	-1.493 -375.7	7.71×10^7	-342	+0.3506	+0.4689	0.0026
					-439	+0.6495	-0.4783	
					-5217 -5309	-0.004780 +0.004690	+0.004804 +0.004626	
IV	9	-2.376 -597.8	-2.035 -512.0	1.08×10^8	-491	+0.1641	+0.3665	0.0018
					-619	+0.8361	-0.3680	
					-5215 -5310	-0.005253 +0.004933	+0.005211 +0.004898	

^aFrom Chezem and Helmick (4), with modifications. See Footnote 1, page 12. and Footnote 1, page 14.

to the roots.¹ Column (9) gives the values of the time t_p of the peak of the response curve $G_2(t)$, computed from the average of α_1 and α_2 .

Figures 1 through 4 give the computed functions $G_1(t)$ and $G_2(t)$ for each of the cases considered in Table 1, drawn as smooth curves from $t = 0$ to $t = 0.010$ sec. Experimental data obtained by Chezem and Helmick are shown by crosses, and the circles are the values of the same functions obtained by the analog whose construction and operation will be described in the next section.

¹It should be pointed out here that in the Chezem-Helmick report (4) Columns (5) and (6) of Table I (page 12) do not show the values of U_1 and V_1 as stated in the headings but the values of AU_1 and AV_1 respectively, and that the first two roots given in Column (7) must be interchanged to conform to the values of R_1 and R_2 as defined by their Equations 8a and 8b, or 8c, which correspond to Equations 12, 13 and 14 respectively in this section.

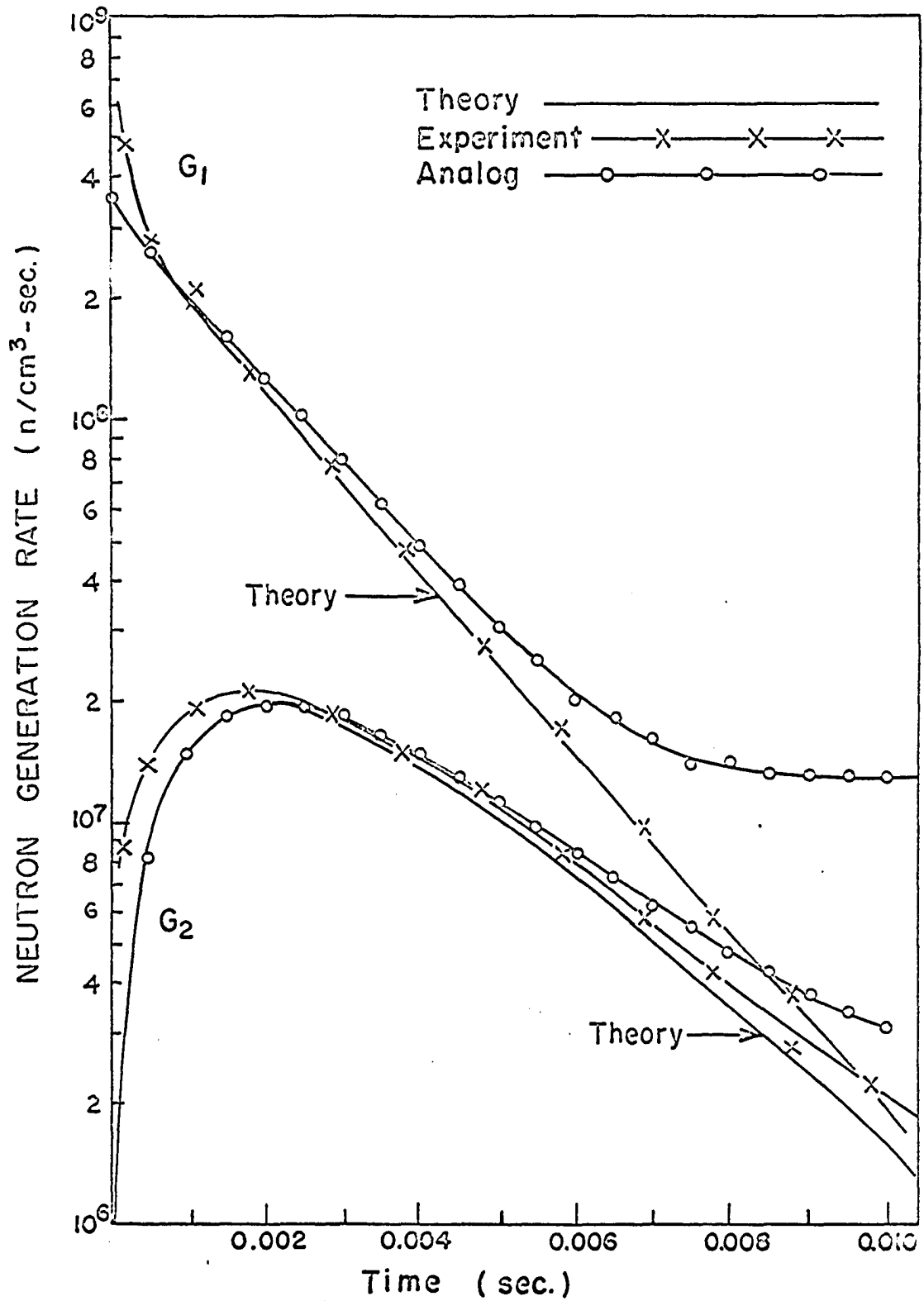


Figure 1. Neutron generation rates for driving and passive cores for Case I

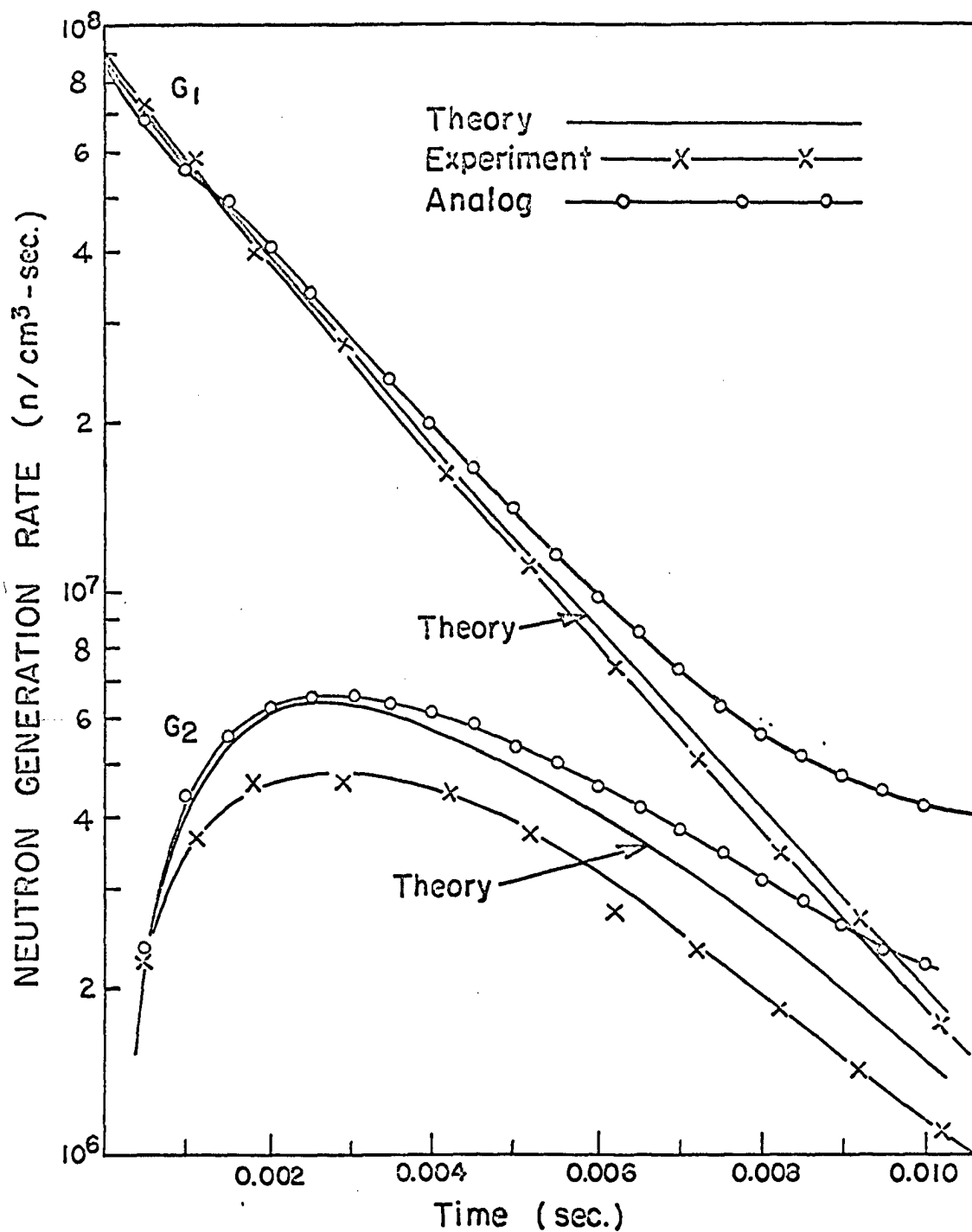


Figure 2. Neutron generation rates for driving and passive cores for Case II

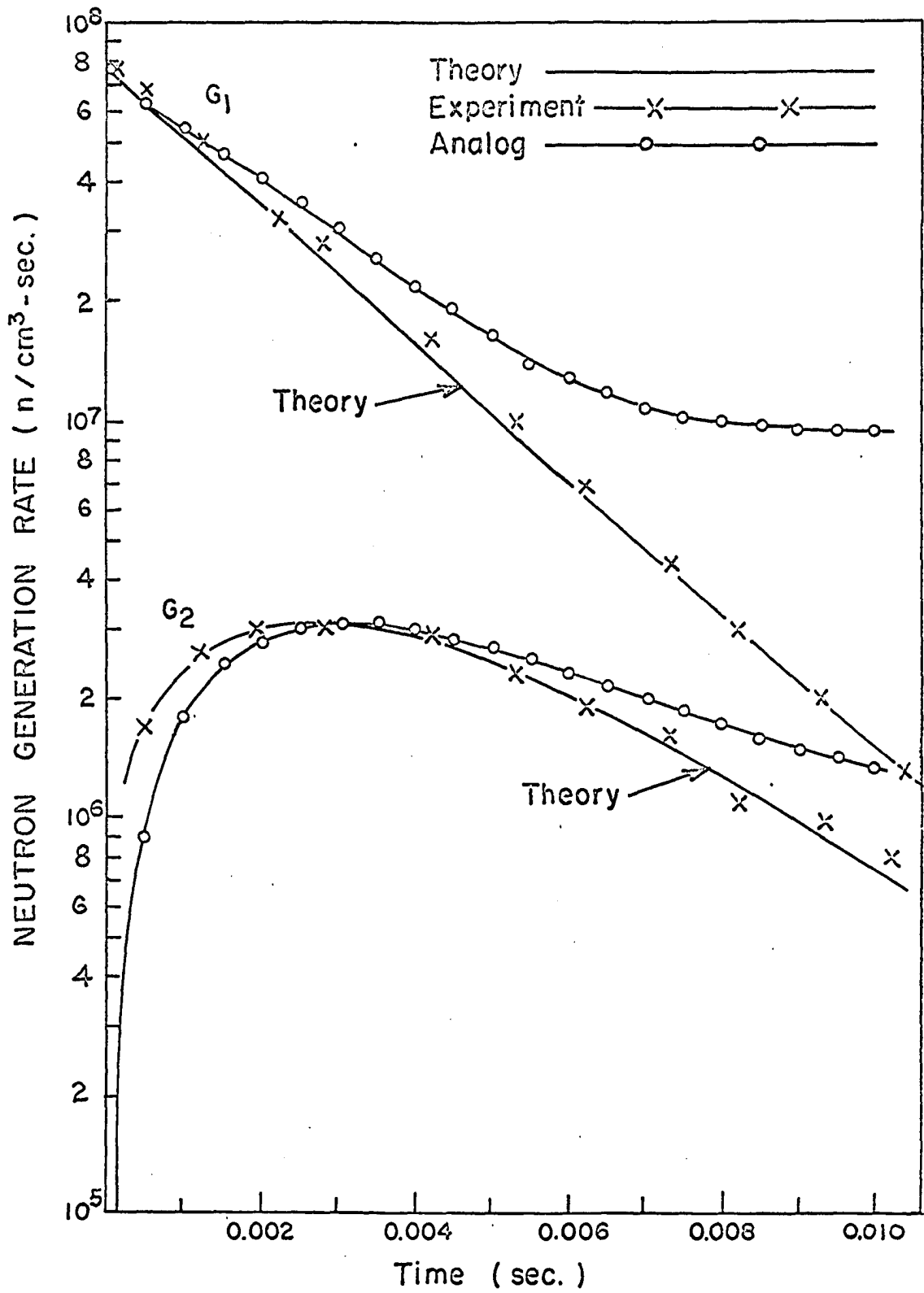


Figure 3. Neutron generation rates for driving and passive cores for Case III

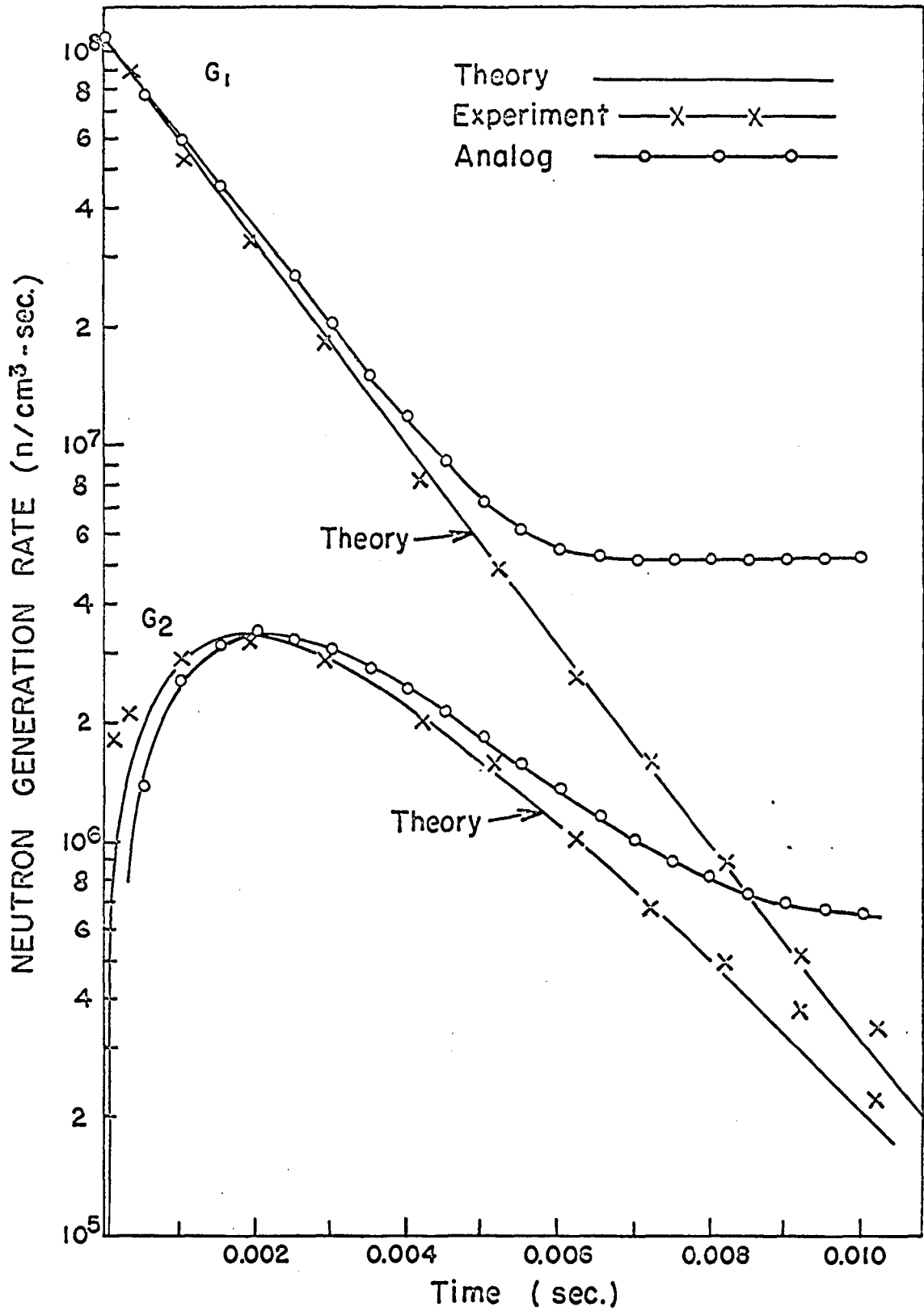


Figure 4. Neutron generation rates for driving and passive cores for Case IV

AN ANALOG SIMULATION OF THE
CHEZEM-HELMICK TWO-CORE MODEL

The primary aim of this study is the construction of an analog to simulate the Chezem-Helmick model of a two-core reactor whose theory was developed in the preceding section. Available are two PACE analog computers each with a maximum of four amplifiers that can be used as integrators, a slave connection between the analog computers and a plotter.

It is proposed to construct an analog simulating the Chezem-Helmick equations. It is convenient to work with these equations in their transfer function form, Equations 7 and 8 in the preceding section, page 8.

$$\frac{g_1(s)}{A} = \frac{(s-\alpha_2)(s+\frac{1}{T})^2}{(s-\alpha_1)(s-\alpha_2)(s+\frac{1}{T})^2 - \gamma^2} . \quad (18)$$

$$\frac{g_2(s)}{A} = \frac{\gamma(s+\frac{1}{T})}{(s-\alpha_1)(s-\alpha_2)(s+\frac{1}{T})^2 - \gamma^2} . \quad (19)$$

The method to be used here is that suggested by Jackson (9, page 223), which is suitable for a case such as this where several outputs have the same denominator.

Define an auxiliary function as

$$g_3(s) = \mathcal{L}\{G_3(t)\} = \frac{A}{(s-\alpha_1)(s-\alpha_2)(s+\frac{1}{T})^2 - \gamma^2} . \quad (20)$$

The functions $g_1(s)$ and $g_2(s)$ can be expressed as linear combinations of this function and its successive derivatives.

$$g_1(s) = [(s - \alpha_2)(s + \frac{1}{\tau})^2] g_3(s)$$

$$g_2(s) = [\gamma(s + \frac{1}{\tau})] g_3(s)$$

Transformation of the Equations

Equations 18 and 19 can be rewritten as

$$\frac{g_1(s)}{A} = \frac{s^3 + K_1 s^2 + K_2 s + K_3}{s^4 + K_4 s^3 + K_5 s^2 + K_6 s + K_7} \quad (21)$$

$$\frac{g_2(s)}{A} = \frac{\gamma s + K_0}{s^4 + K_4 s^3 + K_5 s^2 + K_6 s + K_7} \quad (22)$$

where the coefficients K_i are obtained by algebraic multiplication:

$$K_0 = \frac{\gamma}{\tau} \quad (23)$$

$$K_1 = \frac{2}{\tau} - \alpha_2 \quad (24)$$

$$K_2 = \frac{1}{\tau^2} - \frac{2\alpha_2}{\tau} \quad (25)$$

$$K_3 = -\frac{\alpha_2}{\tau^2} \quad (26)$$

$$K_4 = \frac{2}{\tau} - \alpha_1 - \alpha_2 \quad (27)$$

$$K_5 = \frac{1}{\tau^2} - \frac{2(\alpha_1 + \alpha_2)}{\tau} + \alpha_1 \alpha_2 \quad (28)$$

$$K_6 = \frac{2\alpha_1\alpha_2}{\tau} - \frac{\alpha_1 + \alpha_2}{\tau^2} \quad (29)$$

$$K_7 = \frac{\alpha_1\alpha_2}{\tau^2} - \gamma^2. \quad (30)$$

Hence the auxiliary function $g_3(s)$ required by the Jackson method is

$$g_3(s) = \frac{A}{s^4 + K_4s^3 + K_5s^2 + K_6s + K_7} \quad (31)$$

and it is this function which must first be simulated.

Rewrite Equation 31 as

$$[s^4 + K_4s^3 + K_5s^2 + K_6s + K_7] g_3(s) = A \quad (32)$$

The most convenient method for solving this equation is by treating it as a differential equation.

Solution of Equation 32

Consider the homogeneous differential equation

$$\begin{aligned} \frac{d^4G_3(t)}{dt^4} + K_4 \frac{d^3G_3(t)}{dt^3} + K_5 \frac{d^2G_3(t)}{dt^2} \\ + K_6 \frac{dG_3(t)}{dt} + K_7G_3(t) = 0. \end{aligned} \quad (33)$$

Its complete Laplace transform, assuming non-zero derivatives, is

$$\begin{aligned} [s^4 + K_4s^3 + K_5s^2 + K_6s + K_7] g_3(s) - [s^3 + K_4s^2 + K_5s + K_6]G_3(0) \\ - [s^2 + K_4s + K_5]G_3'(0) - [s + K_4]G_3''(0) - G_3'''(0) = 0. \end{aligned} \quad (34)$$

By simple inspection it is seen that Equation 34 reduces to Equation 32 if $G_3'''(t) = A$ and all the derivatives of lower order and the function itself equal zero initially.¹ Here the solution of the non-homogeneous Equation 32 is replaced by an equivalent operation, the solution of a homogeneous equation with one non-vanishing derivative as initial condition.²

Initial Conditions

At this point in the analysis it is proper to check back to see if the initial conditions assumed in taking the Laplace transforms actually are zero. The assumed initial conditions are that $G_1(0) = 0$ and $G_2(0) = 0$ in Equation 3, and that $G_3(0) = G_3'(0) = G_3''(0) = 0$ in Equation 34. The "initial condition" $G_3'''(0) = A$ with the homogeneous equation $[s^4 + K_4s^3 + K_5s^2 + K_6s + K_7]g_3(s) = 0$ was there taken as replacing the non-homogeneous equation $[s^4 + K_4s^3 + K_5s^2 + K_6s + K_7]g_3(s) = A$ with zero initial conditions. There is no way of knowing before solving these equations whether or not these initial

¹This leads to the conclusion that the Laplace transform of the impulse function is completely analogous to an initial condition on the (n-1)-th derivative in an n-order system, which is a more general statement than that found in Johnson (10, page 124).

²Aseltine (1, pages 22-30) gives a short discussion of the impulse function; specially interesting and relevant to the subject under discussion here is the last section which shows the correlation between initial condition and the impulse function. The impulse function is also treated, adequately for the purposes of this section, in Cheng (3, pages 220-224).

conditions are satisfied, but once they have been solved these can always be checked.

The solutions for $G_1(t)$ and $G_2(t)$ are, from Equations 10 and 11,

$$\frac{G_1(t)}{A} = \sum_{i=1}^4 U_i e^{R_i t} \quad \text{where} \quad U_i = \frac{(R - \alpha_2) \left(R_i + \frac{1}{\tau}\right)^2}{4 \prod_{\substack{j=1 \\ j \neq i}}^4 (R_i - R_j)}$$

$$\text{and} \quad \frac{G_2(t)}{A} = \sum_{i=1}^4 V_i e^{R_i t} \quad \text{where} \quad V_i = \frac{\gamma \left(R_i + \frac{1}{\tau}\right)}{4 \prod_{\substack{j=1 \\ j \neq i}}^4 (R_i - R_j)} .$$

The solution for $G_3(t)$ is easily obtained from its defining Equation 20:

$$\frac{g_3(s)}{A} = \frac{1}{(s - \alpha_1)(s - \alpha_2) \left(s + \frac{1}{\tau}\right)^2 - \gamma^2} = \frac{1}{4 \prod_{i=1}^4 (s - R_i)} ,$$

for the function can be written as a sum of partial fractions of the form

$$\frac{g_3(s)}{A} = \sum_{i=1}^4 \frac{W_i}{s - R_i} \quad (35)$$

whose inverse Laplace transform is

$$\frac{G_3(t)}{A} = \sum_{i=1}^4 W_i e^{R_i t} \quad \text{where} \quad W_i = \frac{1}{4 \prod_{\substack{j=1 \\ j \neq i}}^4 (R_i - R_j)} . \quad (36)$$

To find the initial values of these functions it is best to start with $G_3(t)$; successive differentiation of $G_3(t)$ will give

$$G_3'(t) = A \sum_{i=1}^4 R_i W_i e^{R_i t}$$

$$G_3''(t) = A \sum_{i=1}^4 R_i^2 W_i e^{R_i t}$$

$$G_3'''(t) = A \sum_{i=1}^4 R_i^3 W_i e^{R_i t}$$

and at time $t = 0$,

$$G_3(0) = A \sum_{i=1}^4 W_i$$

$$G_3'(0) = A \sum_{i=1}^4 R_i W_i$$

$$G_3''(0) = A \sum_{i=1}^4 R_i^2 W_i$$

$$G_3'''(0) = A \sum_{i=1}^4 R_i^3 W_i$$

(37)

It is easy to show algebraically (see Appendix B) that the first three summations involved in Equations 37 above are zero, and the fourth, $\sum R_i^3 W_i = 1$; so $G_3(0) = G_3'(0) = G_3''(0) = 0$, and $G_3'''(0) = A$. This result agrees with the initial conditions assumed in Equation 34 to make it equivalent to the nonhomogeneous form, Equation 32, with zero initial conditions.

Next consider the functions $G_1(t)$ and $G_2(t)$ and their derivatives:

$$G_1(t) = A \sum_{i=1}^4 U_i e^{R_i t}$$

$$G_2(t) = A \sum_{i=1}^4 V_i e^{R_i t}$$

$$G_1'(t) = A \sum_{i=1}^4 R_i U_i e^{R_i t}$$

$$G_2'(t) = A \sum_{i=1}^4 R_i V_i e^{R_i t}$$

$$G_1''(t) = A \sum_{i=1}^4 R_i^2 U_i e^{R_i t}$$

$$G_2''(t) = A \sum_{i=1}^4 R_i^2 V_i e^{R_i t}$$

$$G_1'''(t) = A \sum_{i=1}^4 R_i^3 U_i e^{R_i t}$$

$$G_2'''(t) = A \sum_{i=1}^4 R_i^3 V_i e^{R_i t}.$$

Their values at $t = 0$ are

$$G_1(0) = A \sum_{i=1}^4 U_i$$

$$G_2(0) = A \sum_{i=1}^4 V_i$$

$$G_1'(0) = A \sum_{i=1}^4 R_i U_i$$

$$G_2'(0) = A \sum_{i=1}^4 R_i V_i$$

$$G_1''(0) = A \sum_{i=1}^4 R_i^2 U_i$$

$$G_2''(0) = A \sum_{i=1}^4 R_i^2 V_i$$

$$G_1'''(0) = A \sum_{i=1}^4 R_i^3 U_i$$

$$G_2'''(0) = A \sum_{i=1}^4 R_i^3 V_i.$$

The coefficients U_i and V_i can be expressed in terms of

W_i :

$$U_i = (R_i - \alpha_2) \left(R_i + \frac{1}{\tau}\right)^2 W_i$$

$$= \left[R_i^3 + \left(\frac{2}{\tau} - \alpha_2\right) R_i^2 + \left(\frac{1}{\tau^2} - \frac{2\alpha_2}{\tau}\right) R_i - \frac{\alpha_2}{\tau^2} \right] W_i$$

$$\text{and } V_i = \gamma \left(R_i + \frac{1}{\tau}\right) W_i$$

$$= \left(\gamma R_i + \frac{\gamma}{\tau}\right) W_i$$

and the first few summations in Equation 38 then become

$$\Sigma U_i = \Sigma R_i^3 W_i + \left(\frac{2}{T} - \alpha_2\right) \Sigma R_i^2 W_i + \left(\frac{1}{T^2} - \frac{2\alpha_2}{T}\right) \Sigma R_i W_i - \frac{\alpha}{T^2} \Sigma W_i = 1$$

$$\Sigma V_i = \gamma \Sigma R_i W_i + \frac{\gamma}{T} \Sigma W_i = 0,$$

$$\Sigma R_i V_i = \gamma \Sigma R_i^2 W_i + \frac{\gamma}{T} \Sigma R_i W_i = 0,$$

using the results, previously obtained, that $\Sigma W_i = \Sigma R_i W_i = \Sigma R_i^2 W_i = 0$, and $\Sigma R_i^3 W_i = 1$. Hence $G_1(0) = A$ and $G_2(0) = G_2'(0) = 0$, but the other derivatives do not vanish initially. The initial value A for $G_1(t)$ again agrees with the "initial condition" assumed as an alternate method to the Laplace transform of the impulse function.

Analog Solutions

The equation for $g_3(s)$ can now be synthesized on the analog computer. To render the equation into a form suitable for analogical solution, it may be rewritten as follows:

$$s^4 g_3(s) = -[K_4 s^3 + K_5 s^2 + K_6 s + K_7] g_3(s)$$

$$\text{or } s^3 g_3(s) = -\frac{1}{s} [K_4 s^3 + K_5 s^2 + K_6 s + K_7] g_3(s) \quad (39)$$

with the initial condition $G_3'''(0) = A$.

Figure 5 shows the elements and connections for the solution of Equation 39. All coefficients K_i are found to be positive and the diagram is made accordingly. The integrators numbered 1, 3, 5, and 7 in succession at the middle of the diagram give the successive derivatives of $G_3(t)$ and the output of amplifier 7 is then $-G_3(t)$, and that of amplifier 9 is

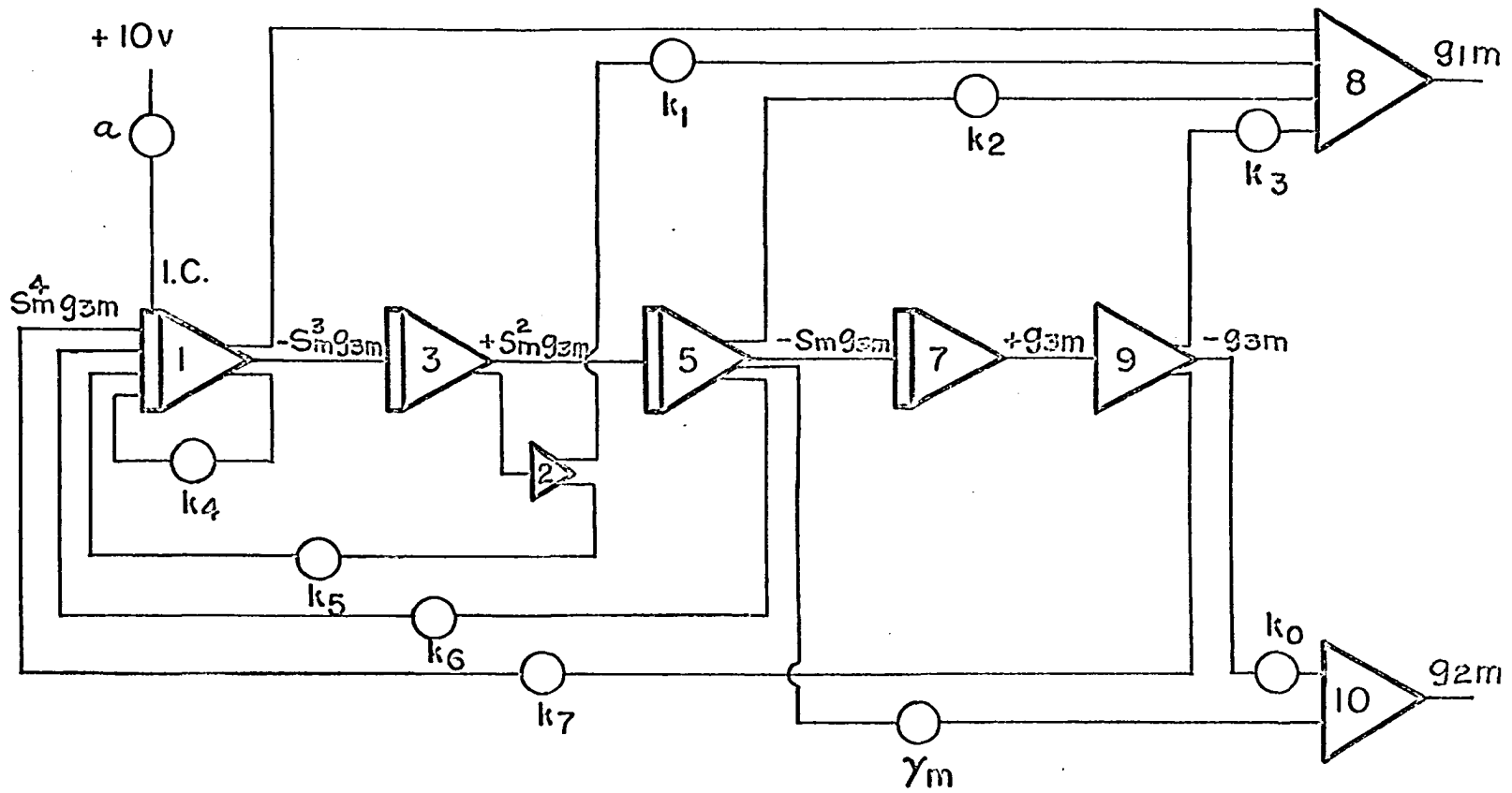


Figure 5. Computer diagram for the Chezem-Helmick model of a two-core reactor

$G_3(t)$, which may be read and plotted if desired. The initial condition on $G_3(t)$ is accounted for in the circuit by a voltage, properly reduced by the factor a from the 10-volt source, connected to the I.C. (initial condition) terminal of amplifier-integrator 1. . . . -

$G_1(t)$ and $G_2(t)$ may now be obtained from $G_3(t)$ by the relations

$$g_1(s) = [s^3 + K_1s^2 + K_2s + K_3]g_3(s) \quad (40)$$

$$\text{and } g_2(s) = [Ys + K_0]g_3(s). \quad (41)$$

To produce the desired variables $G_1(t)$ and $G_2(t)$ on the simulator, the appropriate functions of $G_3(t)$ multiplied by the proper factors as specified by Equations 40 and 41, are summed. The complete circuit is shown also in Figure 5, the summing amplifier shown at the top synthesizing the value of $G_1(t)$ and the one at the bottom of the figure that of $G_2(t)$.

Problem Set-Up and Scaling

The calculations for Case I of the Chezem-Helmick experiment will be outlined here, to illustrate the way this problem is set up and put into the computer. Complete calculations are shown in Appendix A.

The values of Y and of the coefficients K_0 through K_7 computed from Equations 23 through 30 are as follows:

$$Y = 5.923 \times 10^5$$

$$K_0 = 4.556 \times 10^9 \quad -$$

$$\begin{aligned}
K_1 &= 1.590 \times 10^4 \\
K_2 &= 6.714 \times 10^7 \\
K_3 &= 3.067 \times 10^{10} \\
K_4 &= 1.646 \times 10^4 \\
K_5 &= 7.595 \times 10^7 \\
K_6 &= 6.783 \times 10^{10} \\
K_7 &= 1.663 \times 10^{13}.
\end{aligned}$$

The equations to be solved are found by substituting these values for the coefficients in Equations 21 and 22. These are Equations 42 and 43 in Table 2a.

Scaling

To keep the variable voltages corresponding to the different variables and parameters of the problem within the limits of operation of the amplifiers, the variables must be scaled. The computer to be used is the PACE-10 which admits no more than 10 volts for each amplifier. In what follows the machine variable will be represented by placing m as a second subscript beside that of the corresponding problem variable.

From Table 1 and Figure 1 it is seen that $A = 3.63 \times 10^8$, $g_1(\text{max}) = 3.63 \times 10^8$ and $g_2(\text{max}) = 2 \times 10^7$. For a maximum voltage of 10 volts then, make $g_1 = 10^8 g_{1m}$, $g_2 = 10^7 g_{2m}$, and let $A = \rho A_m$ and $\theta t = t_m$. From the last relation, $t = \frac{1}{\theta} t_m$; then $dt = \frac{1}{\theta} dt_m$, so

$$s = \frac{d}{dt} = \theta \frac{d}{dt_m} = \theta s_m \quad \text{and} \quad s^n = \theta^n s_m^n.$$

Make $\theta = 10^4$ and with the other scaling substitutions Equations 38 and 39 become Equations A and B in Table 2b. And with a choice of $\rho = 10^{12}$ they reduce to Equations C and D in the same table.

The machine variable corresponding to the auxiliary function $g_3(s)$ will then be

$$g_{3m}(s) = \frac{A_m}{s_m^4 + 1.646s_m^3 + 0.7595s_m^2 + 0.06783s_m + 0.001663}$$

In summary the equations to be solved on the computer are

$$s_m^3 g_{3m}(s) = -\frac{1}{s_m} [1.646s_m^3 + 0.7595s_m^2 + 0.06783s_m + 0.001663] g_{3m}(s)$$

$$g_{1m}(s) = [s_m^3 + 1.590s_m^2 + 0.6714s_m + 0.03067] g_{3m}(s)$$

$$g_{2m}(s) = [0.5923s_m + 0.4556] g_{3m}(s)$$

The coefficients γ , K_i and A_m in the original equations, transformed by scaling and by the gain on the amplifier connections, are replaced by γ_m , k_i and a in the circuit diagram given here as Figure 5.

Similar computations were made for Cases II, III and IV, and these results with those from Case I are given in Table 3.

The potentiometers are set to the values of the coefficients, according to the scale adopted and gain of each amplifier, and curves are obtained of the outputs of amplifiers 8 and 10 for $G_1(t)$ and $G_2(t)$ respectively. These curves are shown in Figures 6 through 9, and the results read from them have been incorporated into Figures 1 through 4, to compare

Table 2a. Equations 42 and 43

$$\frac{g_1(s)}{A} = \frac{s^3 + (1.590 \times 10^4)s^2 + (6.714 \times 10^7)s + (3.067 \times 10^{10})}{s^4 + (1.646 \times 10^4)s^3 + (7.595 \times 10^7)s^2 + (6.783 \times 10^{10})s + (1.663 \times 10^{13})} \quad (42)$$

$$\frac{g_2(s)}{A} = \frac{(5.923 \times 10^5)s + (4.556 \times 10^9)}{s^4 + (1.646 \times 10^4)s^3 + (7.595 \times 10^7)s^2 + (6.783 \times 10^{10})s + (1.663 \times 10^{13})} \quad (43)$$

Table 2b. Equations A, B, C and D

$$\frac{10^8 g_{1m}}{\rho A_m} = \frac{10^{12} s_m^3 + (1.590 \times 10^{12})s_m^2 + (6.714 \times 10^{11})s_m + (3.067 \times 10^{10})}{10^{16} s_m^4 + (1.646 \times 10^{16})s_m^3 + (7.595 \times 10^{15})s_m^2 + (6.783 \times 10^{14})s_m + (1.663 \times 10^{13})} \quad (A)$$

$$\frac{10^7 g_{2m}}{\rho A_m} = \frac{(5.923 \times 10^9)s + (4.556 \times 10^9)}{10^{16} s_m^4 + (1.646 \times 10^{16})s_m^3 + (7.595 \times 10^{15})s_m^2 + (6.783 \times 10^{14})s_m + (1.663 \times 10^{13})} \quad (B)$$

$$\frac{g_{1m}}{A_m} = \frac{s_m^3 + 1.590s_m^2 + 0.6714s_m + 0.03067}{s_m^4 + 1.646s_m^3 + 0.7595s_m^2 + 0.06783s_m + 0.001663} \quad (C)$$

$$\frac{g_{2m}}{A_m} = \frac{0.5923s_m + 0.4556}{s_m^4 + 1.646s_m^3 + 0.7595s_m^2 + 0.06783s_m + 0.001663} \quad (D)$$

Table 3. Values of the parameters and coefficients for Cases I through IV

Case	I	II	III	IV
β		0.0078		
l		31×10^{-6} sec		
l^*		3.974×10^{-3} sec		
ϵ	0.306 \$		0.169 \$	
τ_1	130×10^{-6} sec		190×10^{-6} sec	
γ	5.923×10^5		2.238×10^5	
δk_1^P	-2.200 \$	-1.630 \$	-1.609 \$	-2.376 \$
δk_2^P	-2.060 \$	-1.527 \$	-1.493 \$	-2.035 \$
α_1	-553.5	-410.1	-404.8	-597.8
α_2	-518.3	-384.2	-375.7	-512.0
A	3.63×10^8	8.85×10^8	7.71×10^8	1.08×10^8
K_0	4.556×10^9	4.556×10^9	1.178×10^9	1.178×10^9
K_1	1.590×10^4	1.577×10^4	1.090×10^4	1.104×10^4
K_2	6.714×10^7	6.508×10^7	3.165×10^7	3.309×10^7
K_3	3.067×10^{10}	2.273×10^{10}	1.041×10^{10}	1.418×10^{10}
K_4	1.646×10^4	1.618×10^4	1.131×10^4	1.164×10^4
K_5	7.595×10^7	7.155×10^7	3.607×10^7	3.969×10^7
K_6	6.783×10^{10}	4.942×10^{10}	2.322×10^{10}	3.397×10^{10}
K_7	1.663×10^{13}	8.973×10^{12}	4.163×10^{12}	8.430×10^{12}

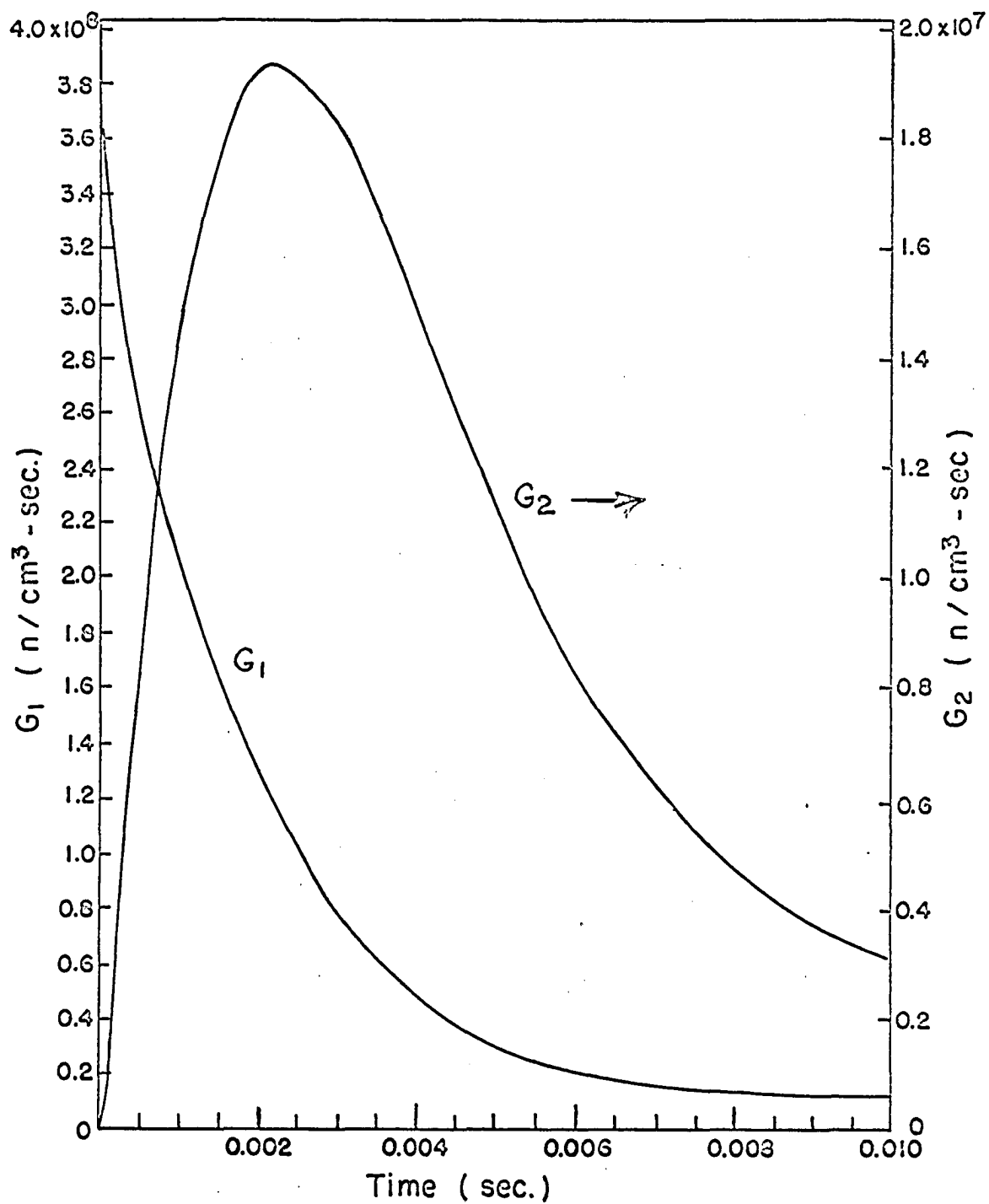


Figure 6. Record of neutron generation rates $G_1(t)$ and $G_2(t)$ from the analog simulation for Case I

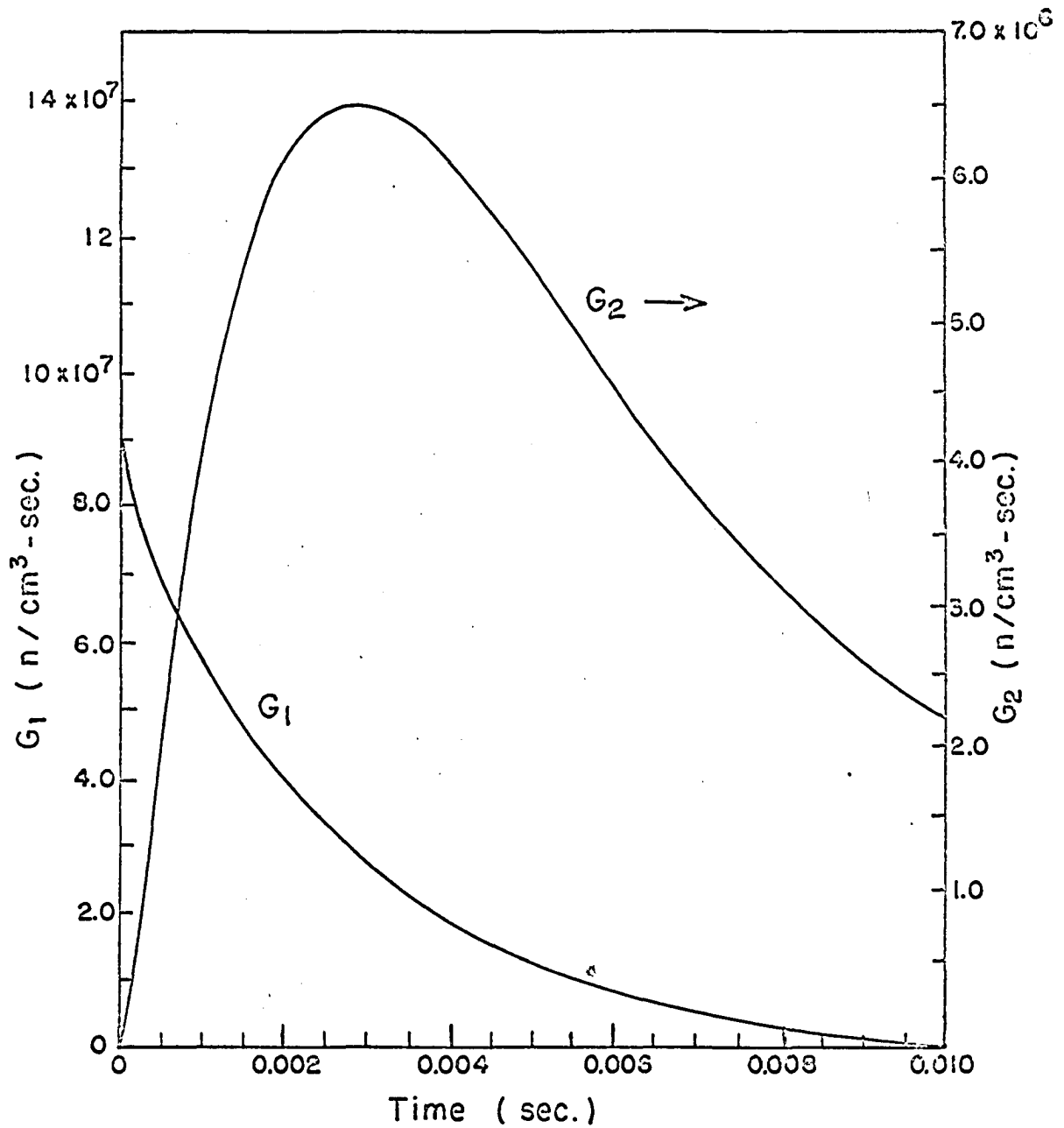


Figure 7. Record of neutron generation rates $G_1(t)$ and $G_2(t)$ from the analog simulation for Case II

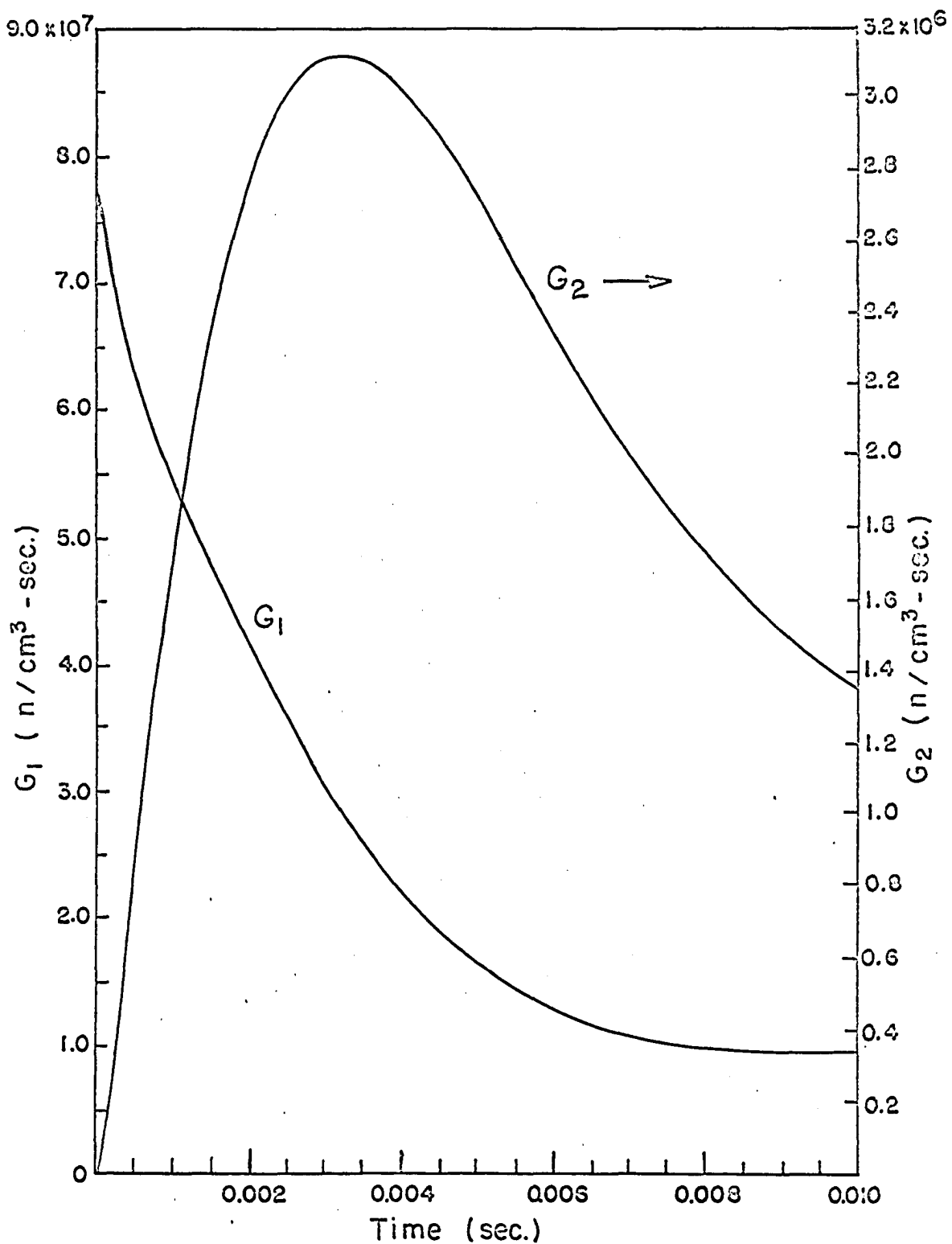


Figure 8. Record of neutron generation rates $G_1(t)$ and $G_2(t)$ from the analog simulation for Case III

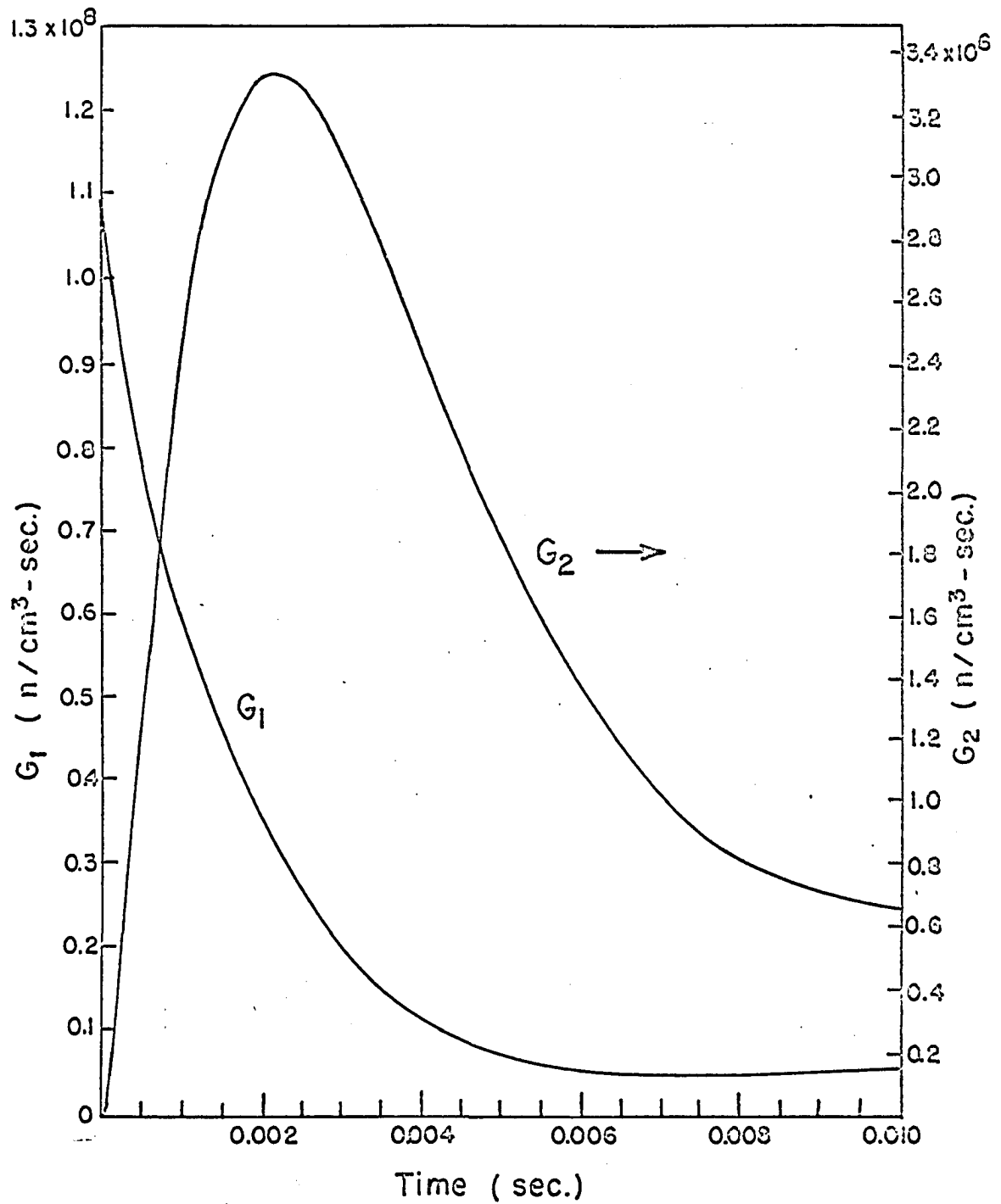


Figure 9. Record of neutron generation rates $G_1(t)$ and $G_2(t)$ from the analog simulation for Case IV

them with the theoretical values and the experimental results of Chezem and Helmick.

Discussion of Results

Figures 1-4 show that, except before the peaks in the functions $G_2(t)$, the analogical results are usually greater than the theoretical values and that they become more and more divergent with time. Table 4 indicates the errors of the analog results, expressed as fractions of the theoretical values, at the ends of four equal time intervals distributed evenly throughout the time-range of the experiment.

Table 4. Relative error in the analog readings

Case Time msec	I		II		III		IV	
	G_1	G_2	G_1	G_2	G_1	G_2	G_1	G_2
2.5	0.08	0.02	0.05	0.03	0.25	0.02	0.09	0.04
5.0	0.22	0.10	0.10	0.07	0.50	0.12	0.28	0.14
7.5	0.50	0.16	0.28	0.20	2.00	0.30	3.00	0.50
10.0	0.90	1.00	1.02	0.20	3.00	0.50	10.00	1.00

Examination of the above table will reveal that in general the error in $G_2(t)$ is much less than in $G_1(t)$. An explanation for this fact is that the two main terms in the function $G_2(t)$ are positive and negative, while those in $G_1(t)$ are both positive, so that the errors inherent in the analog amplifiers tend to cancel in G_2 while they add in G_1 .

Up to a time of 5 milliseconds (50 seconds of machine time) the errors are less than 30% except in one instance. Analog computers are to be used for a machine time of from 20 to 30 seconds, and for this limiting time the errors can be made to fall within a value of 10%, which is usually taken as an average figure for analog computations.

Because the simulator is based on the theory, the values predicted by it for times less than 2 milliseconds, before the peak in G_2 is reached, are usually closer to the theoretical values than those obtained in Chezem and Helmick's experiment. At the start of the experiment the system is sensitive to room-scattered neutrons and this is how the authors explain the results at short times.¹

The tentative conclusion reached then is that the analog suggested in this work is adequate to reproduce the predictions of the Chezem-Helmick theory to within the limits reasonable for the kind of simulators being used and to about the same accuracy as the theory predicts the results of experiment, except for a short interval after the start of the experiment.

In the next section this simulator will be used to study a simple problem that could arise in an analysis of two-core reactor systems: to find the effect on the neutron generation rates of variations in reactivity in both the driven and the passive cores.

¹See Chezem and Helmick (4, page 11).

AN APPLICATION OF THE ANALOG SIMULATOR

Effect of Reactivity Drops
on Neutron Generation Rates

The analog simulator developed in the preceding section will now be used in analyzing a problem that might arise in two-core reactor design: to find the effect, on the neutron generation rates, of reactivity changes in the pulsed and in the passive cores. To consider a definite situation, the two cores will be assumed as in the configuration of Case I of the Chezem-Helmick experiment; the values of the parameters and some useful constants for this case are¹

$$\beta = 0.0078$$

$$l = 31 \times 10^{-6} \text{ sec}$$

$$l^* = 3.974 \times 10^{-3} \text{ sec}$$

$$\epsilon = 0.306 \text{ \$}$$

$$\tau = 130 \times 10^{-6} \text{ sec}$$

$$\gamma = 5.923 \times 10^5$$

$$A = 3.63 \times 10^8$$

$$K_0 = \frac{\gamma}{\tau} = 4.556 \times 10^9.$$

The reactivities in the two cores will be assumed to change by constant steps, which here will be taken arbitrarily as a numerical multiple of the coupling coefficient $\epsilon = 0.306 \text{ \$}$ between the two cores when six feet apart. Four reactivity-drop

¹Chezem and Helmick (4, page 8).

values will be considered for each core: -0.612 , -1.224 , -2.448 , -3.672 , which will be designated by the numerals 1, 2, 3, 4 respectively for Core No. 1 the driving core, and by A, B, C, D respectively for Core No. 2, the passive core. A particular case will therefore be denoted by a number and a letter, for example, 1A, 1B, ..., 2A, ..., 3A, ..., 4A, ... 4D.

The coefficients K_1 for each of these cases are computed as in the second section, from Equations 23 through 30. The details of the computation are similar to those shown in Appendix A for Case I of the Chezem-Helmick experiment and are not shown here. The resulting coefficients are given in Table 5.

The coefficients K_1 and A_m , modified by the scaling factors and the gains of the respective amplifiers, are set on the corresponding potentiometers according to the computer circuit diagram shown in Figure 5, as was done before, and curves of the neutron generation rates $G_1(t)$ and $G_2(t)$ are obtained for the 16 cases. The curves are shown in Figures 10, 11, 12 and 13 for varying δk_2^P , and in Figures 14, 15, 16 and 17 for varying δk_1^P . These figures are traces from the actual graphs obtained from the plotter.

The figures show that the generation rate $G_2(t)$ in the passive core falls with increasing negative reactivity changes, as expected. The reverse effect is shown in the

values will be considered for each core: -0.612 , -1.224 , -1.836 , -2.448 , which will be designated by the numerals 1, 2, 3, 4 respectively for Core No. 1 the driving core, and by A, B, C, D respectively for Core No. 2, the passive core. A particular case will therefore be denoted by a number and a letter, for example, 1A, 1B, ..., 2A, ..., 3A, ..., 4A, ... 4D.

The coefficients K_1 for each of these cases are computed as in the second section, from Equations 23 through 30. The details of the computation are similar to those shown in Appendix A for Case I of the Chezem-Helmick experiment and are not shown here. The resulting coefficients are given in Table 5.

The coefficients K_1 and A_m , modified by the scaling factors and the gains of the respective amplifiers, are set on the corresponding potentiometers according to the computer circuit diagram shown in Figure 5, as was done before, and curves of the neutron generation rates $G_1(t)$ and $G_2(t)$ are obtained for the 16 cases. The curves are shown in Figures 10, 11, 12 and 13 for varying δk_2^P , and in Figures 14, 15, 16 and 17 for varying δk_1^P . These figures are traces from the actual graphs obtained from the plotter.

The figures show that the generation rate $G_2(t)$ in the passive core falls with increasing negative reactivity changes, as expected. The reverse effect is shown in the

Table 5. Parameters and coefficients in the analog study of effect of reactivity drops on neutron generation rates

Case 1. $\delta k_1^P = -0.612\beta$

$\alpha_1 = -154.0$

	A	B	C	D
δk_2^P	-0.612 β	-1.224 β	-2.448 β	-3.672 β
α_2	-154.0	-308.0	-616.0	-924.0
K_1	1.554x10 ⁴	1.569x10 ⁴	1.600x10 ⁴	1.631x10 ⁴
K_2	6.154x10 ⁷	6.391x10 ⁷	6.865x10 ⁷	7.339x10 ⁷
K_3	0.9122x10 ¹⁰	1.822x10 ¹⁰	3.645x10 ¹⁰	5.467x10 ¹⁰
K_4	1.569x10 ⁴	1.585x10 ⁴	1.615x10 ⁴	1.646x10 ⁴
K_5	6.394x10 ⁷	6.633x10 ⁷	7.111x10 ⁷	7.590x10 ⁷
K_6	1.859x10 ¹⁰	2.807x10 ¹⁰	4.702x10 ¹⁰	6.597x10 ¹⁰
K_7	0.105x10 ¹³	0.246x10 ¹³	0.526x10 ¹³	0.807x10 ¹³

Case 2. $\delta k_1^P = -1.224\beta$

$\alpha_1 = -308.0$

	A	B	C	D
δk_2^P	-0.612 β	-1.224 β	-2.448 β	-3.672 β
α_2	-154.0	-308.0	-616.0	-924.0
K_1	1.554x10 ⁴	1.569x10 ⁴	1.600x10 ⁴	1.631x10 ⁴
K_2	6.154x10 ⁷	6.391x10 ⁷	6.865x10 ⁷	7.339x10 ⁷
K_3	0.9112x10 ¹⁰	1.822x10 ¹⁰	3.645x10 ¹⁰	5.467x10 ¹⁰
K_4	1.585x10 ⁴	1.600x10 ⁴	1.631x10 ⁴	1.662x10 ⁴
K_5	7.111x10 ⁷	7.358x10 ⁷	7.850x10 ⁷	8.343x10 ⁷
K_6	4.702x10 ¹⁰	5.759x10 ¹⁰	7.853x10 ¹⁰	9.987x10 ¹⁰
K_7	0.526x10 ¹³	1.087x10 ¹³	2.210x10 ¹³	3.332x10 ¹³

Table 5. (Continued)

Case 3. $\delta k_1^P = -2.448\beta$

$\alpha_1 = -616.0$

	A	B	C	D
δk_2^P	-0.612 β	-1.224 β	-2.448 β	-3.672 β
α_2	-154.0	-308.0	-616.0	-924.0
K_1	1.554×10^4	1.569×10^4	1.600×10^4	1.631×10^4
K_2	6.154×10^7	6.391×10^7	6.685×10^7	7.339×10^7
K_3	0.9112×10^{10}	1.822×10^{10}	3.645×10^{10}	5.467×10^{10}
K_4	1.615×10^4	1.631×10^4	1.662×10^4	1.692×10^4
K_5	7.111×10^7	7.358×10^7	7.850×10^7	8.343×10^7
K_6	4.702×10^{10}	5.759×10^{10}	7.853×10^{10}	9.987×10^{10}
K_7	0.526×10^{13}	1.087×10^{13}	2.210×10^{13}	3.332×10^{13}

Case 4. $\delta k_1^P = -3.672\beta$

$\alpha_1 = -924.0$

	A	B	C	D
δk_2^P	-0.612 β	-1.224 β	-2.448 β	-3.672 β
α_2	-154.0	-308.0	-616.0	-924.0
K_1	1.554×10^4	1.569×10^4	1.600×10^4	1.631×10^4
K_2	6.154×10^7	6.391×10^7	6.865×10^7	7.339×10^7
K_3	0.9112×10^{10}	1.822×10^{10}	3.645×10^{10}	5.467×10^{10}
K_4	1.646×10^4	1.662×10^4	1.692×10^4	1.723×10^4
K_5	7.590×10^7	7.841×10^7	8.343×10^7	8.846×10^7
K_6	6.597×10^{10}	7.727×10^{10}	9.987×10^{10}	12.25×10^{10}
K_7	0.807×10^{13}	1.649×10^{13}	3.332×10^{13}	5.016×10^{13}

Figure 10. Neutron generation rates $G_1(t)$ and $G_2(t)$ for $\delta k_1^P = -0.612\beta$, Cases 1A, 1B, 1C and 1D, where A, B, C, and D represent $\delta k_2^P = -0.612\beta$, -1.224β , -2.448β and -3.672β , respectively

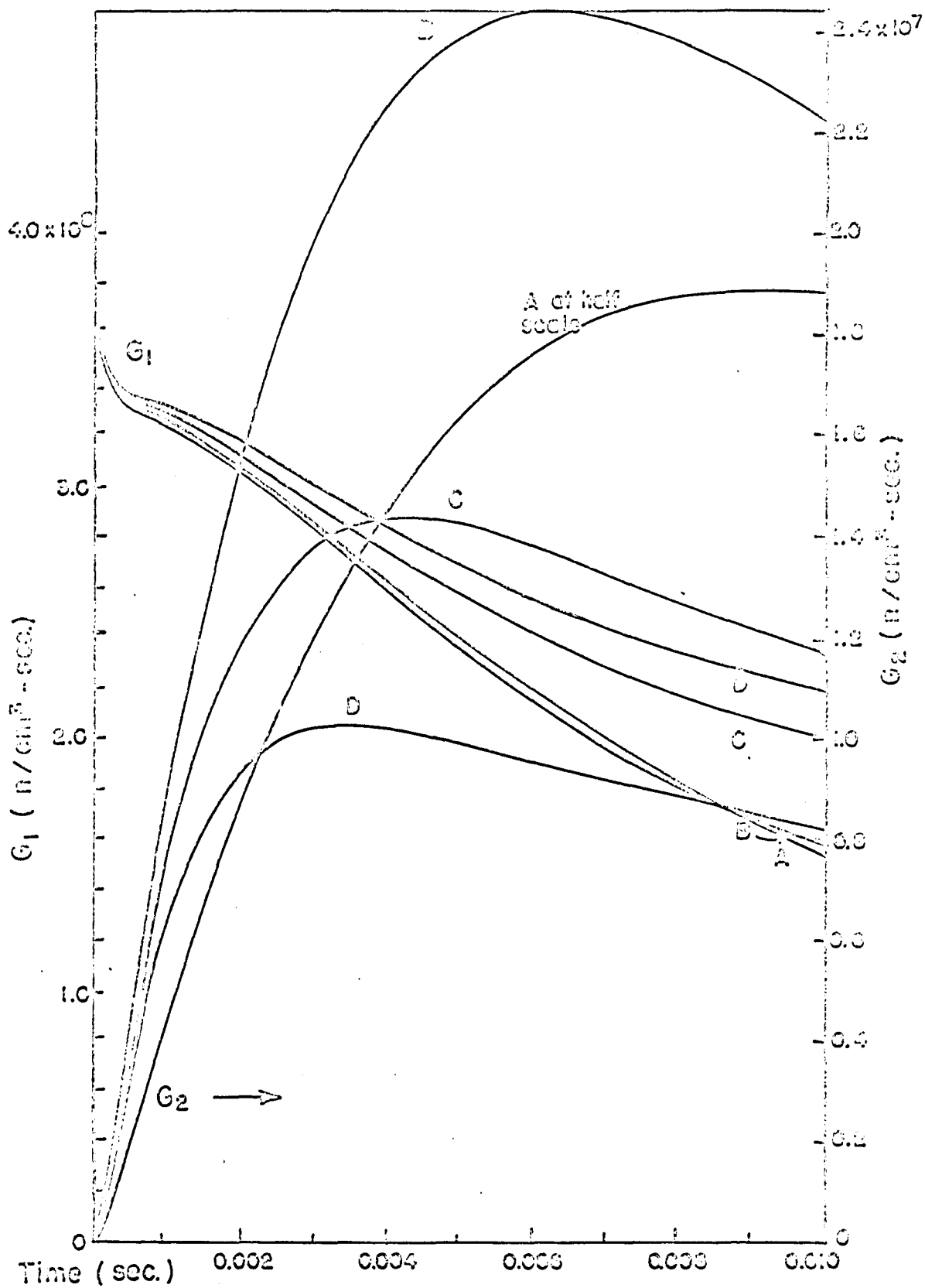


Figure 11. Neutron generation rates $G_1(t)$ and $G_2(t)$ for $\delta k_1^P = -1.224\beta$, Cases 2A, 2B, 2C and 2D, where A, B, C and D represent $\delta k_2^P = -0.612\beta$, -1.224β , -2.44β and -3.672β , respectively

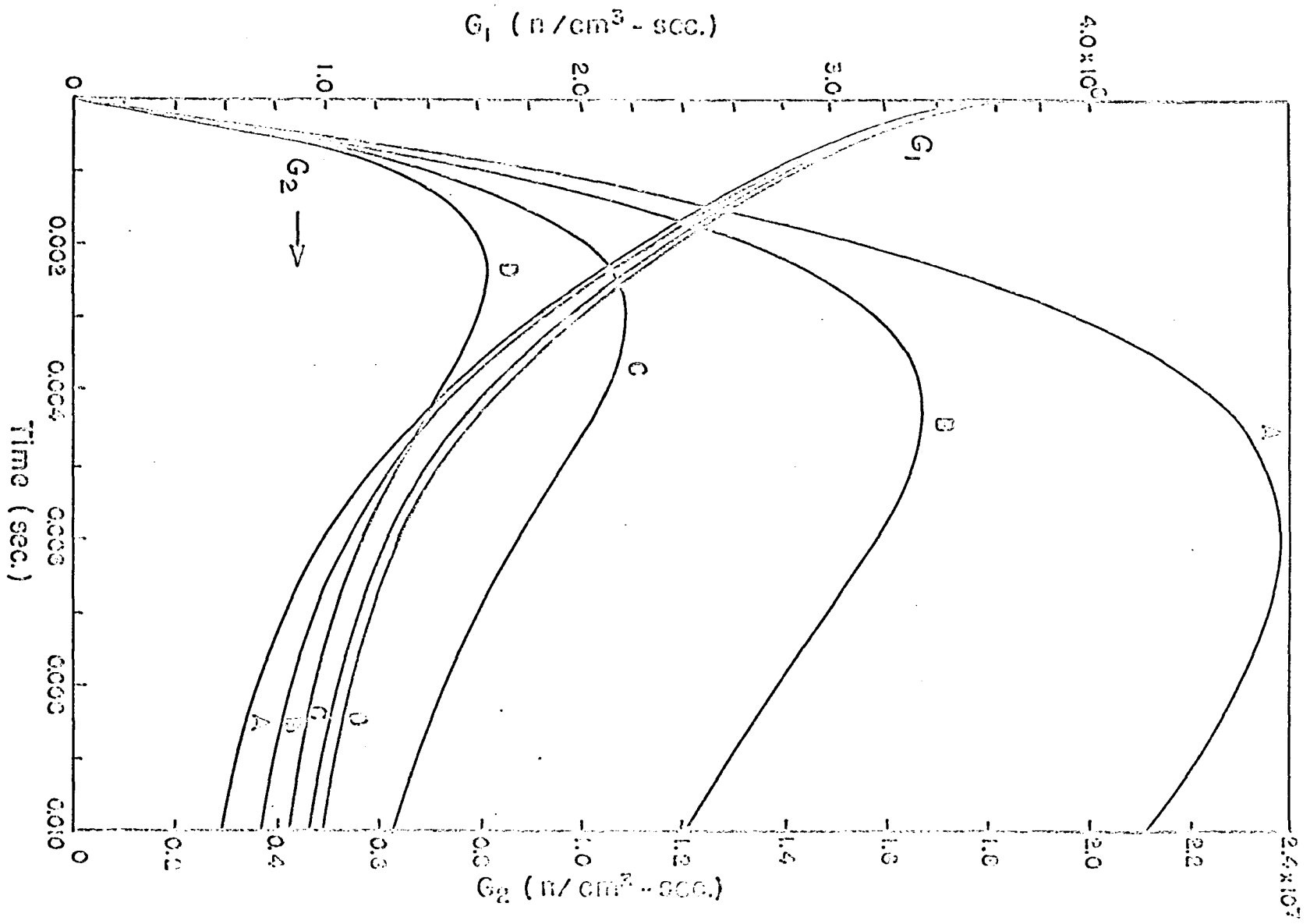


Figure 12. Neutron generation rates $G_1(t)$ and $G_2(t)$ for $\delta k_1^P = -2.448\beta$, Cases 3A, 3B, 3C and 3D, where A, B, C, and D represent $\delta k_2^P = -0.612\beta$, -1.224β , -2.448β and -3.672β , respectively

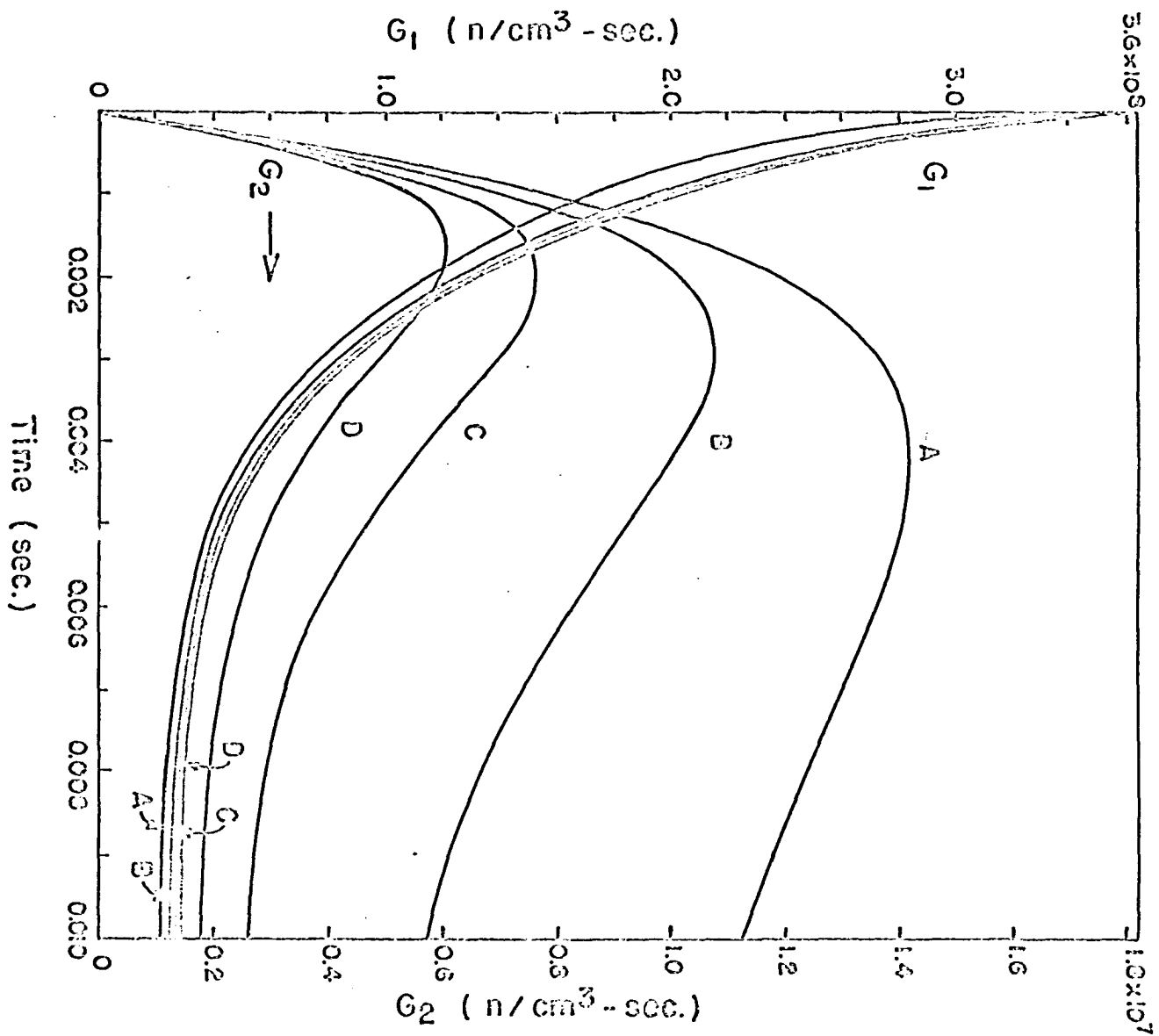


Figure 13. Neutron generation rates $G_1(t)$ and $G_2(t)$ for $\delta k_1^P = -3.672\beta$, Cases 4A, 4B, 4C and 4D, where A, B, C and D represent $\delta k_2^P = -0.612\beta$, -1.224β , -2.448β and -3.672β , respectively

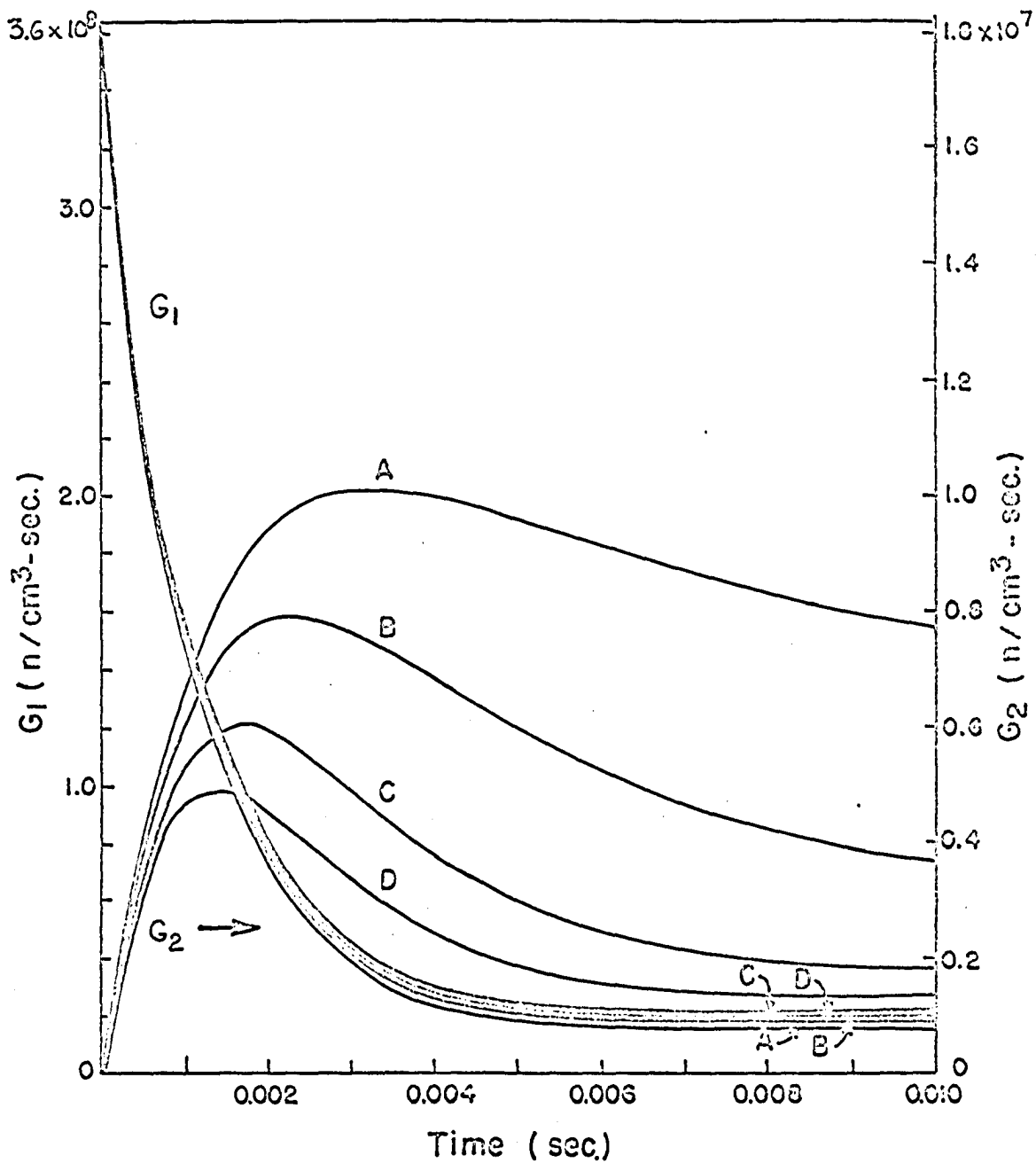


Figure 14. Neutron generation rates $G_1(t)$ and $G_2(t)$ for $\delta k_2^P = -0.612\beta$, Cases 1A, 2A, 3A and 4A, where 1, 2, 3 and 4 represent $\delta k_1^P = -0.612\beta$, -1.224β , -2.448β and -3.672β , respectively

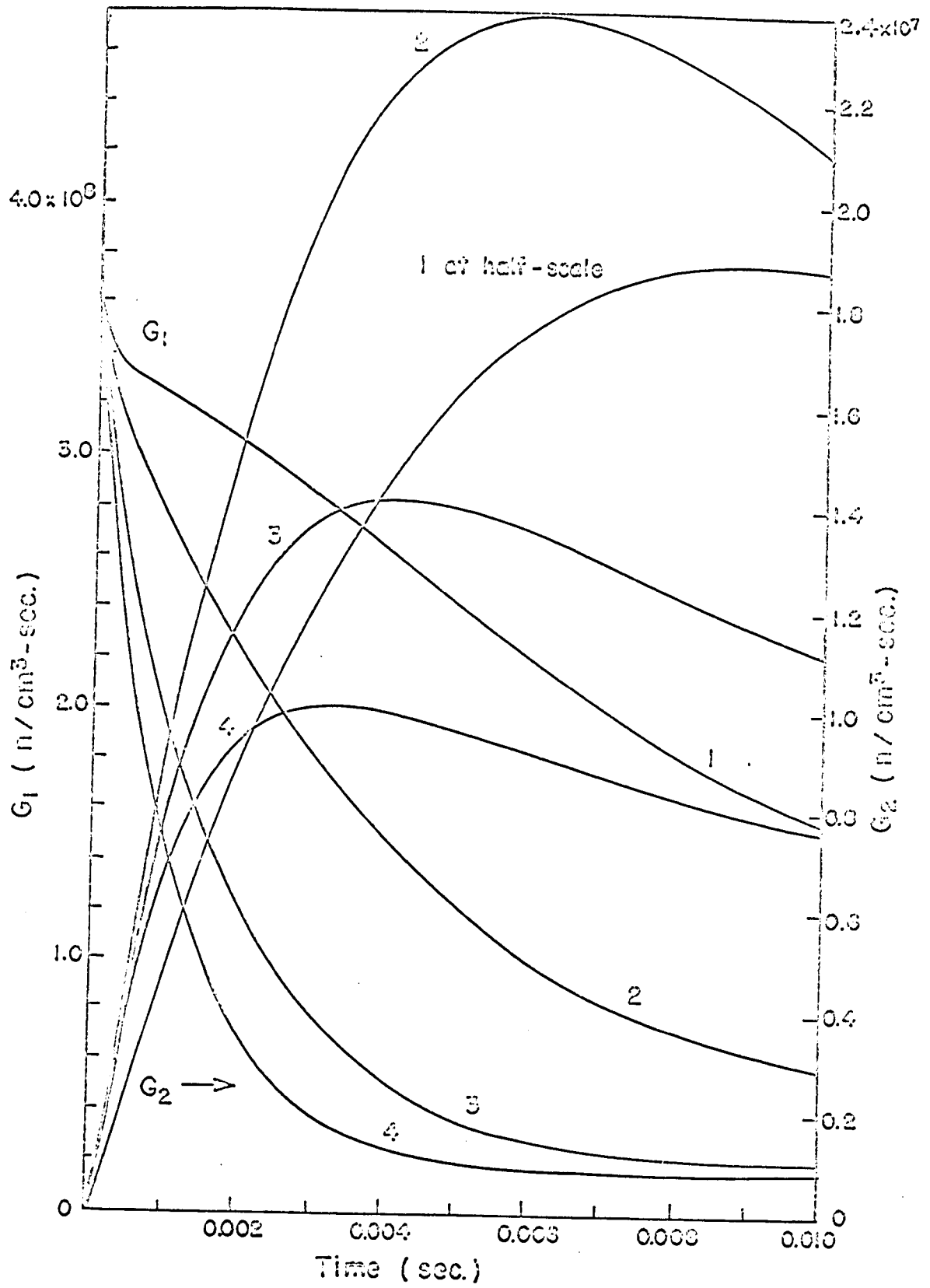


Figure 15. Neutron generation rates $G_1(t)$ and $G_2(t)$ for $\delta k_2^P = -1.224\beta$, Cases 1B, 2B, 3B and 4B, where 1, 2, 3 and 4 represent $\delta k_1^P = -0.612\beta$, -1.224β , -2.448β and -3.672β , respectively

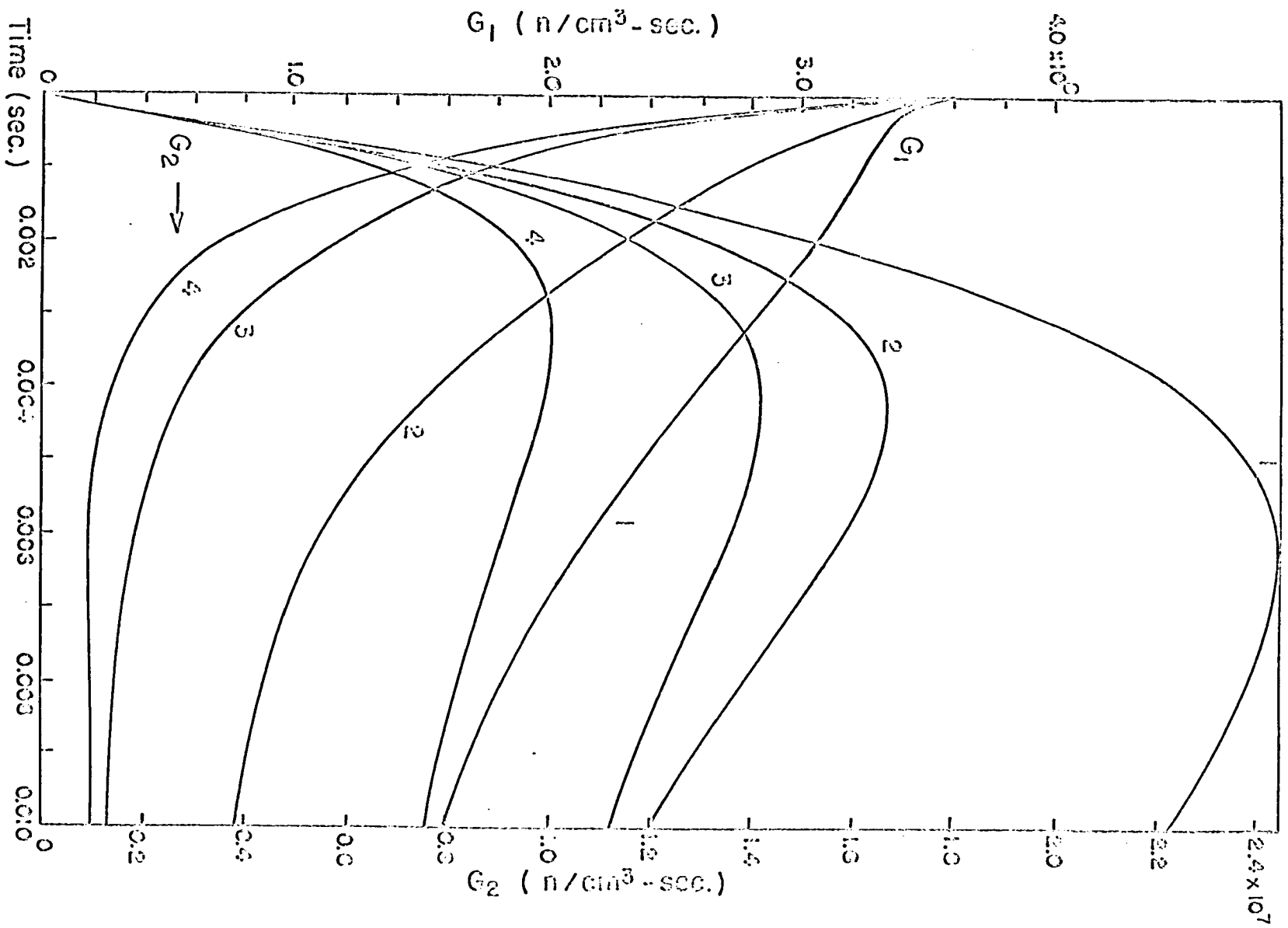


Figure 16. Neutron generation rates $G_1(t)$ and $G_2(t)$ for $\delta k_2^P = -2.448\beta$, Cases 1C, 2C, 3C and 4C, where 1, 2, 3 and 4 represent $\delta k_1^P = -0.612\beta$, -1.224β , -2.448β and -3.672β , respectively

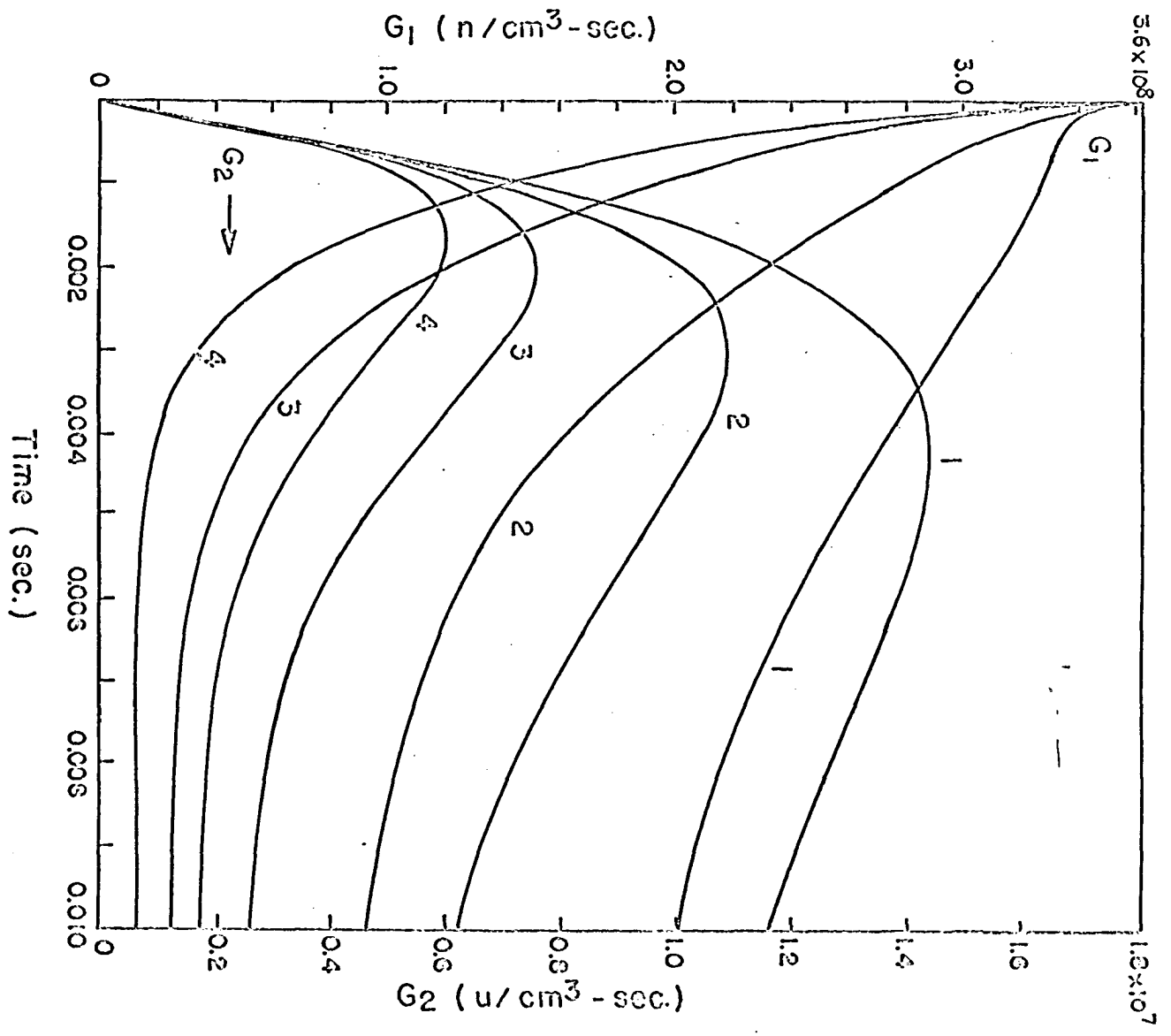
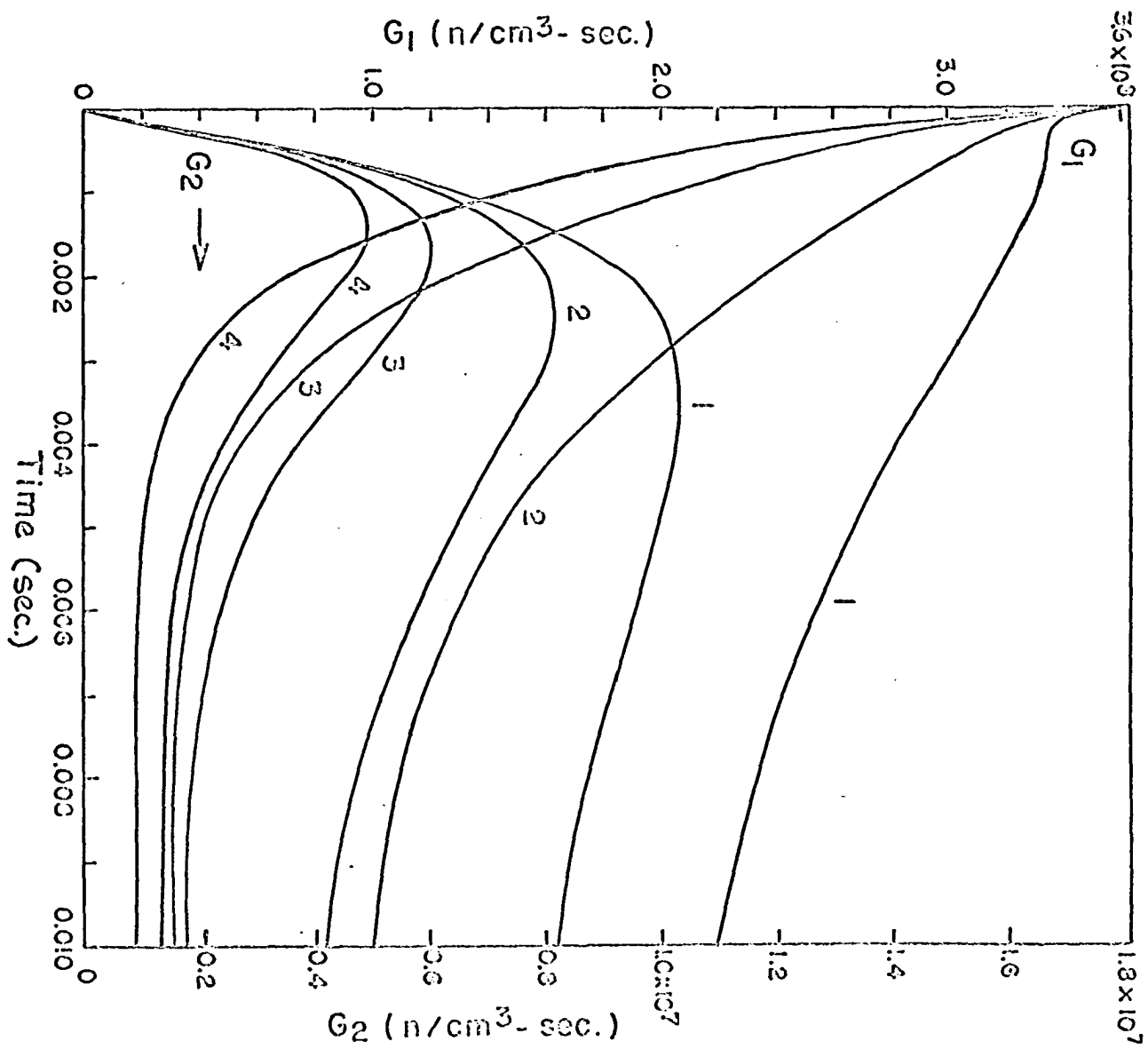


Figure 17. Neutron generation rates $G_1(t)$ and $G_2(t)$ for $\delta k_2^P = -3.672\beta$, Cases 1D, 2D, 3D and 4D, where 1, 2, 3 and 4 represent $\delta k_1^P = -0.612\beta$, -1.224β , -2.448β and -3.672β , respectively



curves for $G_1(t)$ when δk_2^P is varied; then the value of the neutron generation rate in the pulsed core increases with increasing negative reactivity changes. Since this is a result that would not be expected from the usual mechanistic picture of neutron collision, scattering and fission processes, this matter should be looked into further.

It was pointed out in the preceding section that the amplifier errors add in $G_1(t)$ and so it is reasonable to suspect that the unexpected result indicated above, which is contrary to accepted models, might be the result of cumulative amplifier errors. To check this hypothesis a set of three related cases will be examined in more detail.

Take the curves for $G_1(t)$ in cases 1B, 1C and 1D where this abnormal effect is most clearly shown, whose neutronic behavior is given by the simulator as in Figure 10. To determine whether or not the curves shown there are what would be obtained theoretically, the differential equations must be solved exactly. Their solution requires finding the roots of the denominator in Equation 20 when equated to zero, and the difficulty in solving a complete quartic equation makes this approach tedious and impractical.

Solution of the Exact Differential

Equations (Four Roots)

However, useful information may be obtained by taking three cases differing only slightly from 1B, 1C and 1D by

taking as the roots of the denominator those given by Equations 12 and 13, or 14 and 15. Let the resulting cases be denoted by primes: 1B', 1C', 1D'. The complete calculations for the first case, 1B', are given in Appendix C. The coefficients for these cases are shown in Table 6, and the solutions of these in the analog simulator are as shown in Figure 18. Comparison of the values in Tables 5 (Cases 1B, 1C and 1D) with those in Table 6 show small differences, which demonstrate that the exact differential equations being considered in this section are really close to those considered in the preceding one.

The curves show the same trend found earlier, that the neutron generation rate in the pulsed core increases when the reactivity in the other core drops. This is an indication that the simulator here developed fails in this case. Comparison with the theoretical values shows that in all cases the analog values are greater than the theoretical values, evidently due to the accumulated positive errors from the amplifiers.

To obtain an idea of the magnitude of these errors and how they are distributed over the four terms in the solution, the solution will next be studied more closely.

Of the four terms in the result, it is seen by inspection that the contributions of the third and fourth terms (from the τ -dominated roots) are much smaller than those of the first

Table 6. Coefficients for the analog solution of the exact differential equations (four roots)

$$\delta k_1^P = -0.612$$

$$\alpha_1 = -154.0$$

	1B'	1C'	1D'
δk_2^P	-1.224	-2.448	-3.672
α_2	-308.0	-616.0	-924.0
K_1	1.569×10^4	1.600×10^4	1.631×10^4
K_2	6.334×10^7	6.864×10^7	7.347×10^7
K_3	1.822×10^{10}	3.645×10^{10}	5.468×10^{10}
K_4	1.585×10^4	1.616×10^4	1.646×10^4
K_5	6.633×10^7	7.112×10^7	7.591×10^7
K_6	2.815×10^{10}	4.702×10^{10}	6.599×10^{10}
K_7	0.246×10^{13}	0.532×10^{13}	0.814×10^{13}

and second terms (from the Rossi- α -dominated roots), and a quick calculation shows the ratio of the magnitudes to be of the order of 10^{-3} or smaller. Hence it might prove instructive to consider another set of equations retaining only the first terms (that is, with only two roots in its characteristic equation), and see how the analog simulator will solve this case.

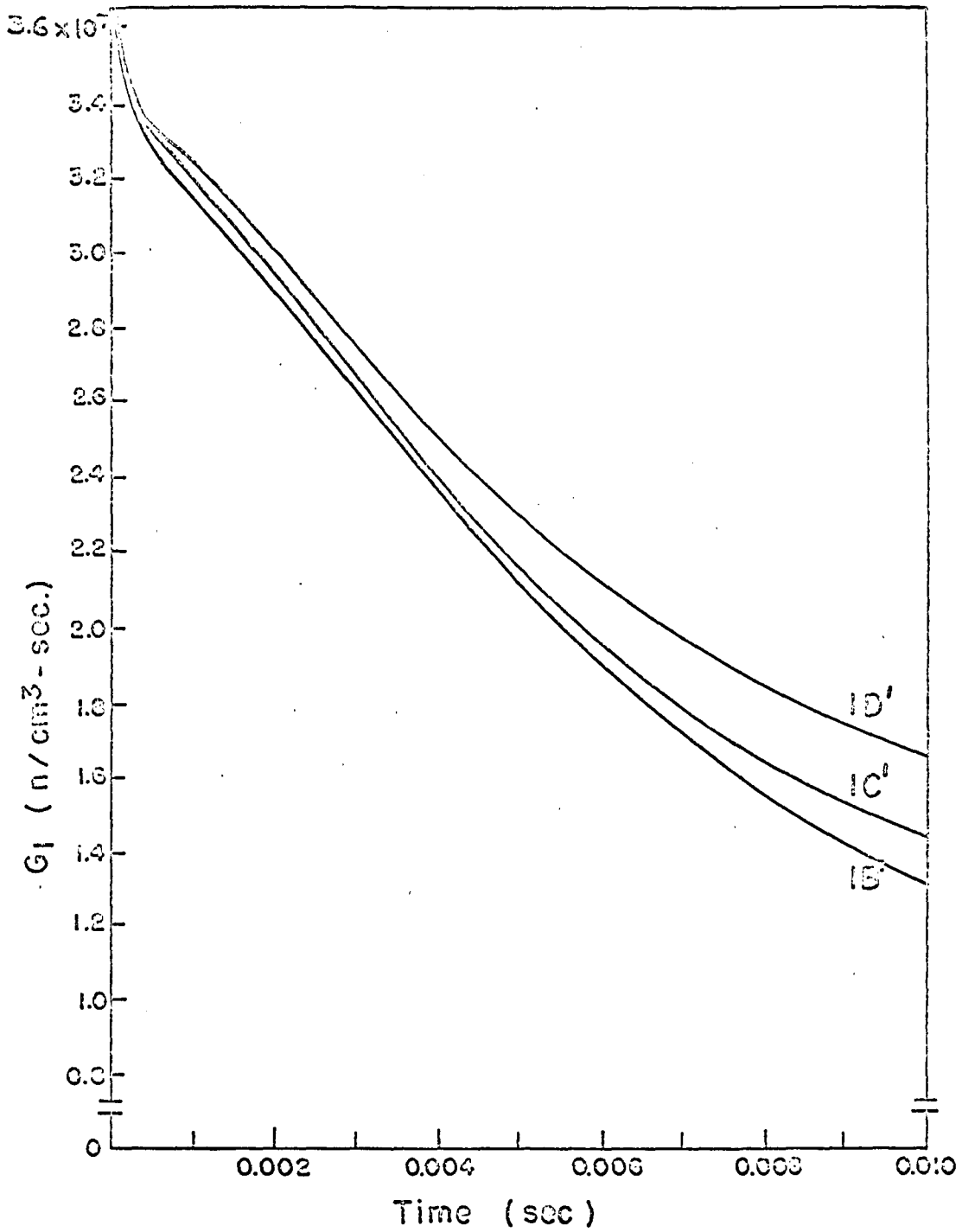


Figure 18. Neutron generation rates $G_1(t)$ for Cases 1B', 1C', 1D'

Solution of the Exact Differential Equations

(Two Roots)

The equations to be solved, in their transfer function form, are

$$\frac{g_1(s)}{A} = \frac{U_1}{s-R_1} + \frac{U_2}{s-R_2} \quad (44)$$

and

$$\frac{g_2(s)}{A} = \frac{V_1}{s-R_1} + \frac{V_2}{s-R_2} \quad (45)$$

The first may be transformed algebraically as shown below:

$$\begin{aligned} \frac{g_1(s)}{A} &= \frac{U_1}{s-R_1} + \frac{U_2}{s-R_2} \\ &= \frac{U_1s - U_1R_2 + U_2s - U_2R_1}{(s-R_1)(s-R_2)} \\ &= \frac{(U_1 + U_2)s + (-U_1R_2 - U_2R_1)}{s^2 + (-R_1 - R_2)s + R_1R_2} \end{aligned}$$

or
$$\frac{g_1(s)}{A} = \frac{M_1s + M_2}{s^2 + M_5s + M_6} \quad (46)$$

In a similar way it can be shown that

$$\frac{g_2(s)}{A} = \frac{M_3s + M_4}{s^2 + M_5s + M_6} \quad (47)$$

In the above Equations 46 and 47

$$M_1 = U_1 + U_2$$

$$M_2 = -U_1R_2 - U_2R_1$$

$$M_3 = V_1 + V_2$$

$$M_4 = -V_1R_2 - V_2R_1$$

$$M_5 = -R_1 - R_2$$

$$M_6 = R_1 R_2$$

Analog simulation

The equations to be solved in the analog computer are then

$$\frac{g_1(s)}{A} = \frac{M_1 s + M_2}{s^2 + M_5 s + M_6}$$

$$\frac{g_2(s)}{A} = \frac{M_3 s + M_4}{s^2 + M_5 s + M_6} .$$

To solve these, let

$$\frac{g_3(s)}{A} = \frac{1}{s^2 + M_5 s + M_6} . \quad (48)$$

Then $g_1(s) = (M_1 s + M_2) g_3(s)$

and $g_2(s) = (M_3 s + M_4) g_3(s)$.

To find $G_3(t)$:

$$\begin{aligned} (s^2 + M_5 s + M_6) g_3(s) &= 0, & G_3'(0) &= A \\ s^2 g_3(s) &= -(M_5 s + M_6) g_3(s) \\ s g_3(s) &= -\frac{1}{s} (M_5 s + M_6) g_3(s) \end{aligned}$$

The circuit diagram for an analog computer to solve the Equations 46 and 47, through the use of the auxiliary variable defined in Equation 48, is shown in Figure 19. The integrators 1 and 3 give $G_3(t)$ and its first derivative, and linear combinations of these are made up to form $G_1(t)$ and $G_2(t)$.

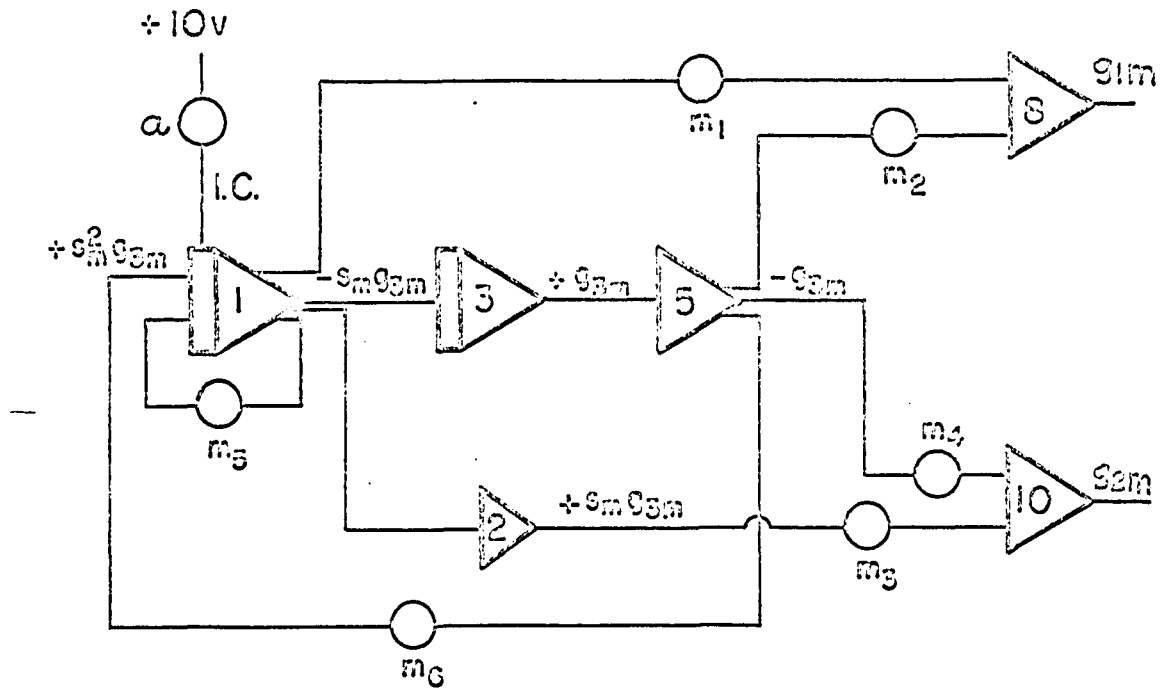


Figure 19. Computer diagram for the solution of the reduced differential equations, Cases 1B", 1C", and 1D"

These functions will be the outputs of amplifiers 8 and 10 respectively.

The shortened equations will be designated with double primes: 1B", 1C", 1D". A typical calculation (for case 1B") is shown in Appendix D. Table 7 gives the coefficients M_i in Equations 46 and 47 for the three cases 1B", 1C", and 1D". And the solutions of these cases for $G_1(t)$, obtained from the analog simulator, are shown in Figure 20. The curves obtained are very close to the theoretical values, obtained from the known solutions of the differential equations.

Table 7. Coefficients for the analog solution of the exact differential equations (two roots)

	1B"	1C"	1D"
M_1	1.000	1.000	1.000
M_2	308.0	616.1	924.2
M_3	- 0.01065	- 0.01110	- 0.01162
M_4	76.95	76.88	76.80
M_5	463.7	771.8	1080
M_6	3.984×10^4	8.875×10^4	13.64×10^4

Effect of the Coefficients K_i

The two related questions may be asked. How sensitive is the simulator to variations in the coefficients K_i ? To what degree would an error in setting up the values of the coefficients on the potentiometers affect the curves?

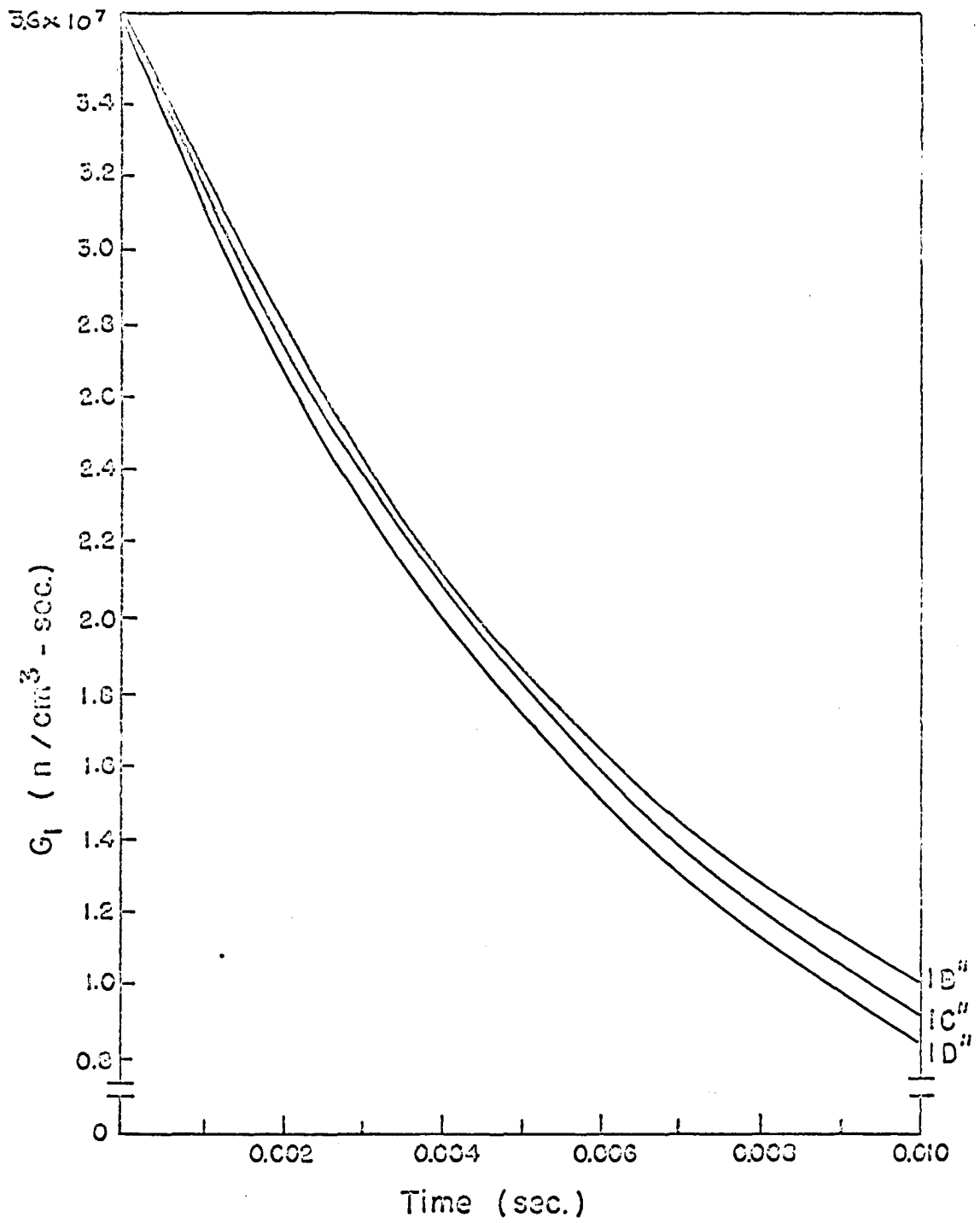


Figure 20. Neutron generation rates $G_1(t)$ for Cases 1B'', 1C'', 1D''

To answer these questions in the present instance case 1B' was run a number of times, each time with a different value of one of the coefficients K_1 . The graphs obtained are shown in Figures 21 through 27, corresponding to variations in K_1 , K_2 , ... K_7 respectively.

The coefficients K_3 and K_7 have the greatest effect on the shapes of the curves, while K_1 and K_4 have little or no effect except within one millisecond after the start. However, the fact that these curves have been shown to be different by making small variations in the values of the coefficients is an indication that manual setting of the potentiometers, guided by visual checking of the values to about 2 parts in 1,000, gives reasonably accurate results, and this cannot be taken as a source of the errors noted earlier.

Summary of Results

A comparison of the analog solutions of the two sets of differential equations will show the relative accuracy with which the analog simulator developed here can give results. Typical data are given in Table 8 for the two sets, together with theoretical values and the differences or errors. The exact equations (primed) show about the same magnitude of errors as the original set (unprimed) to which they are very close as shown earlier, but the reduced-order equations (double-primed) show considerably less error.

Figure 21. Effect of different values of K_1 on the curve of $G_1(t)$

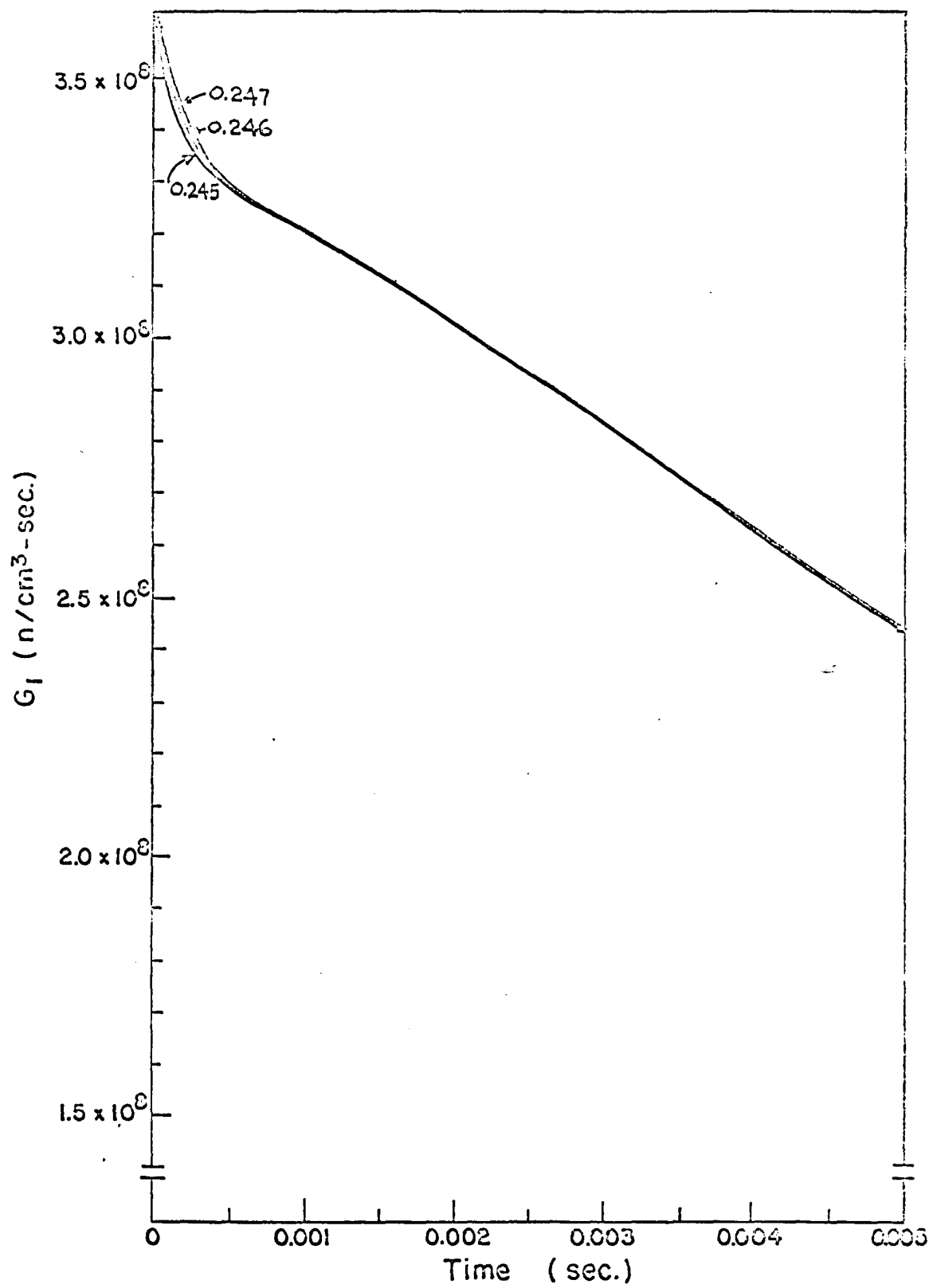


Figure 22. Effect of different values of K_2 on the curve of $G_1(t)$

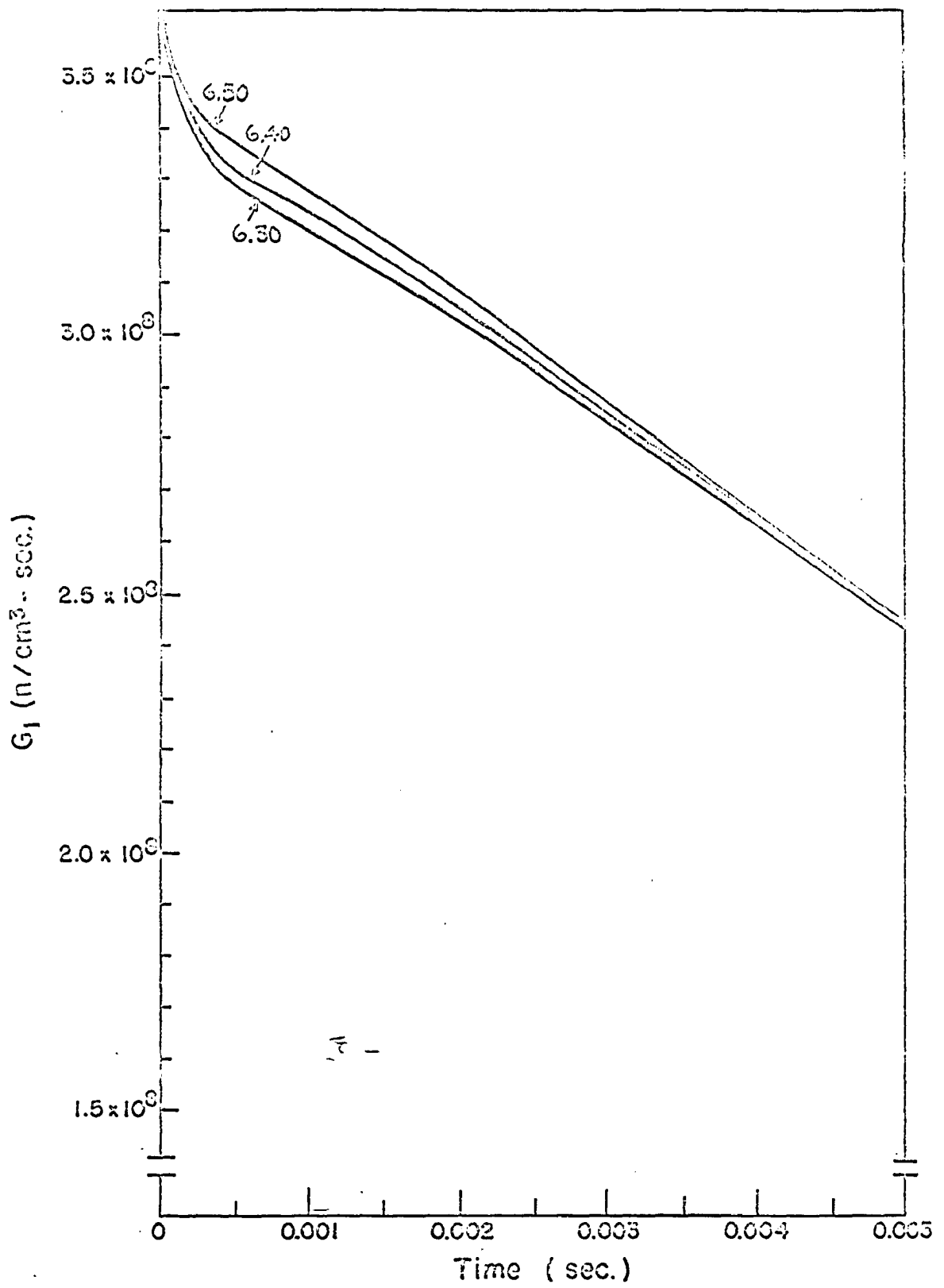


Figure 23. Effect of different values of K_3 on the curve of $G_1(t)$

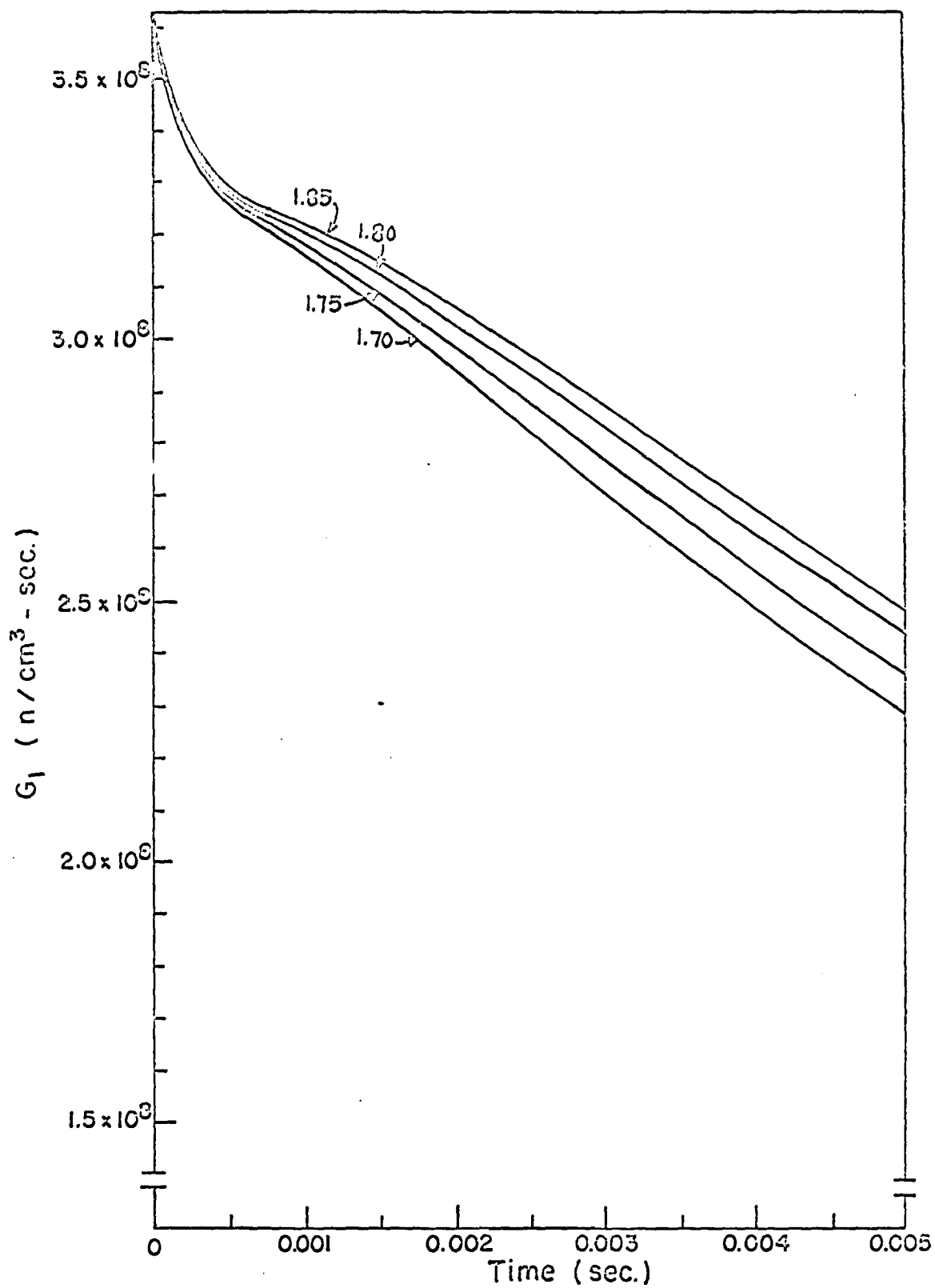


Figure 24. Effect of different values of K_4 on the curve of $G_1(t)$

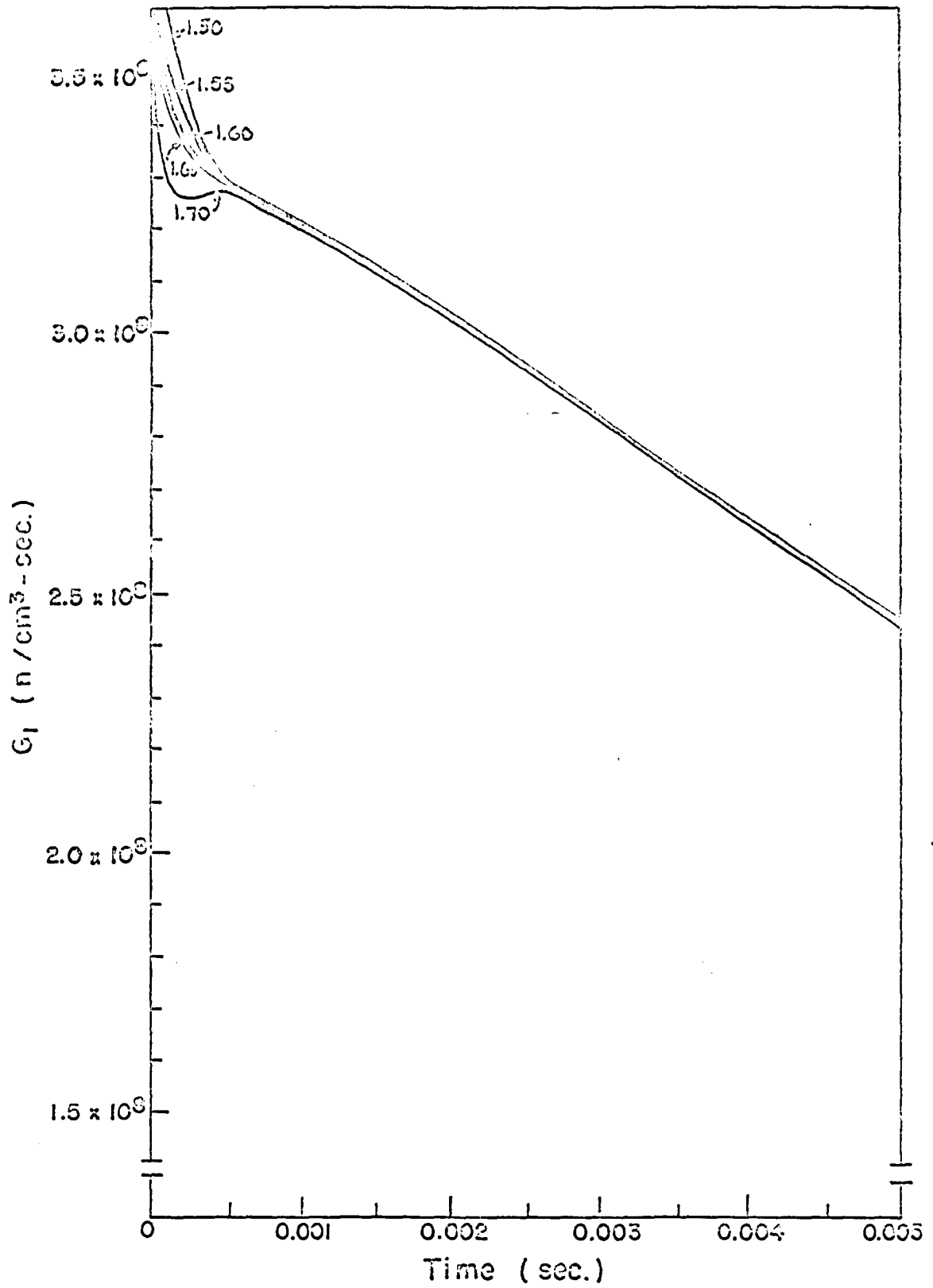


Figure 25. Effect of different values of K_5 on the curve of $G_1(t)$

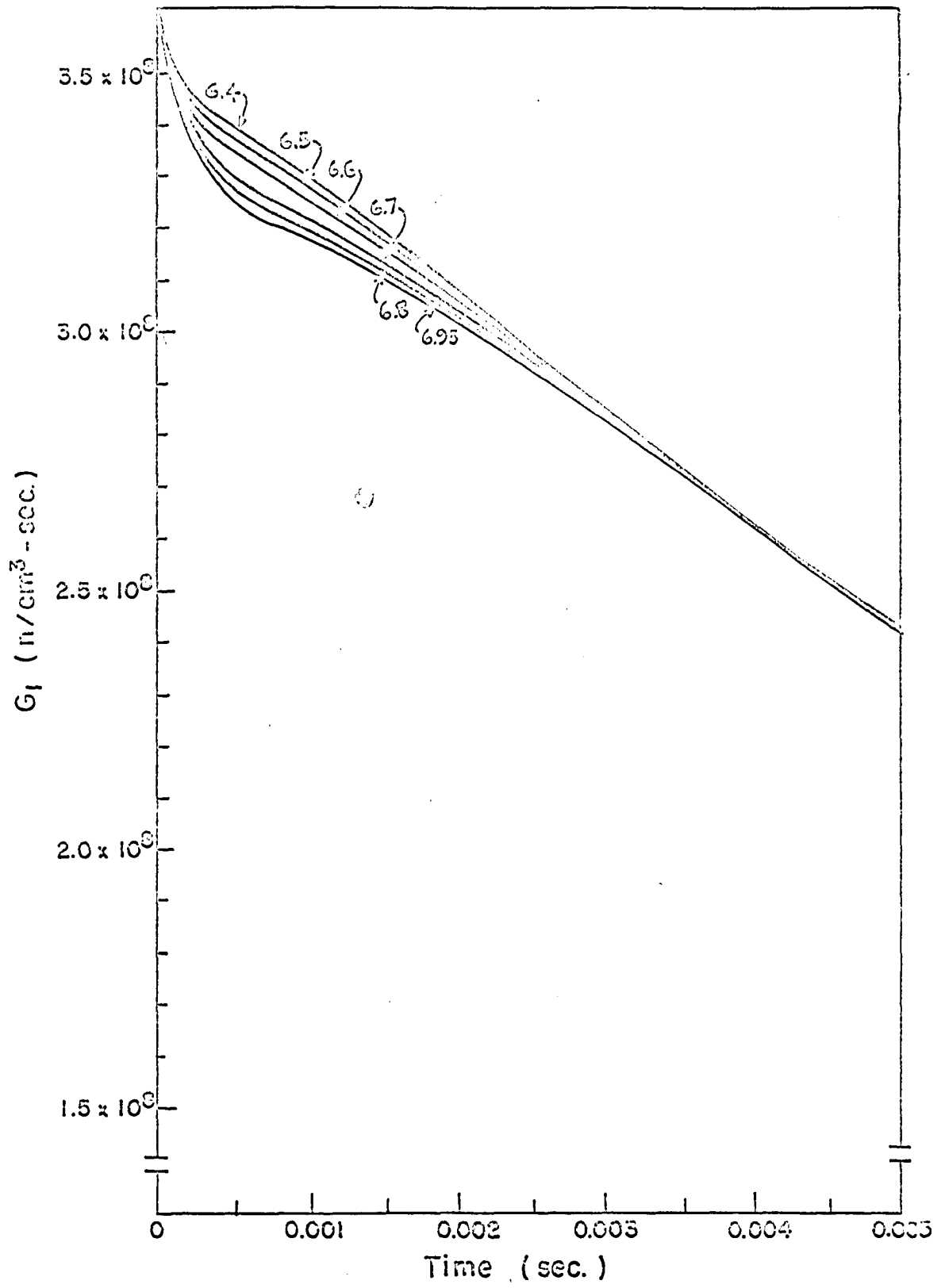


Figure 26. Effect of different values of K_6 on the curve of $G_1(t)$

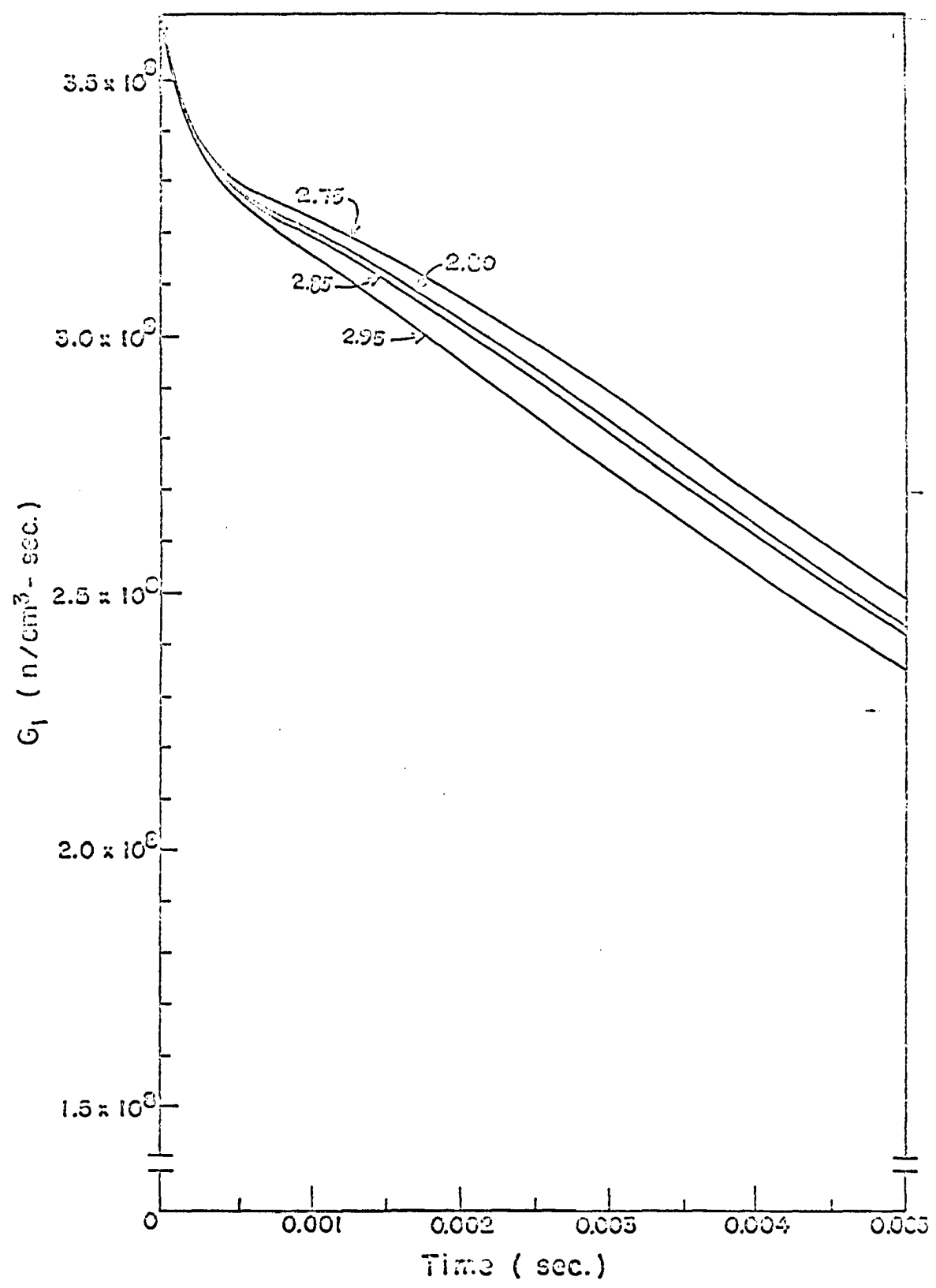


Figure 27. Effect of different values of K_7 on the curve of $G_1(t)$

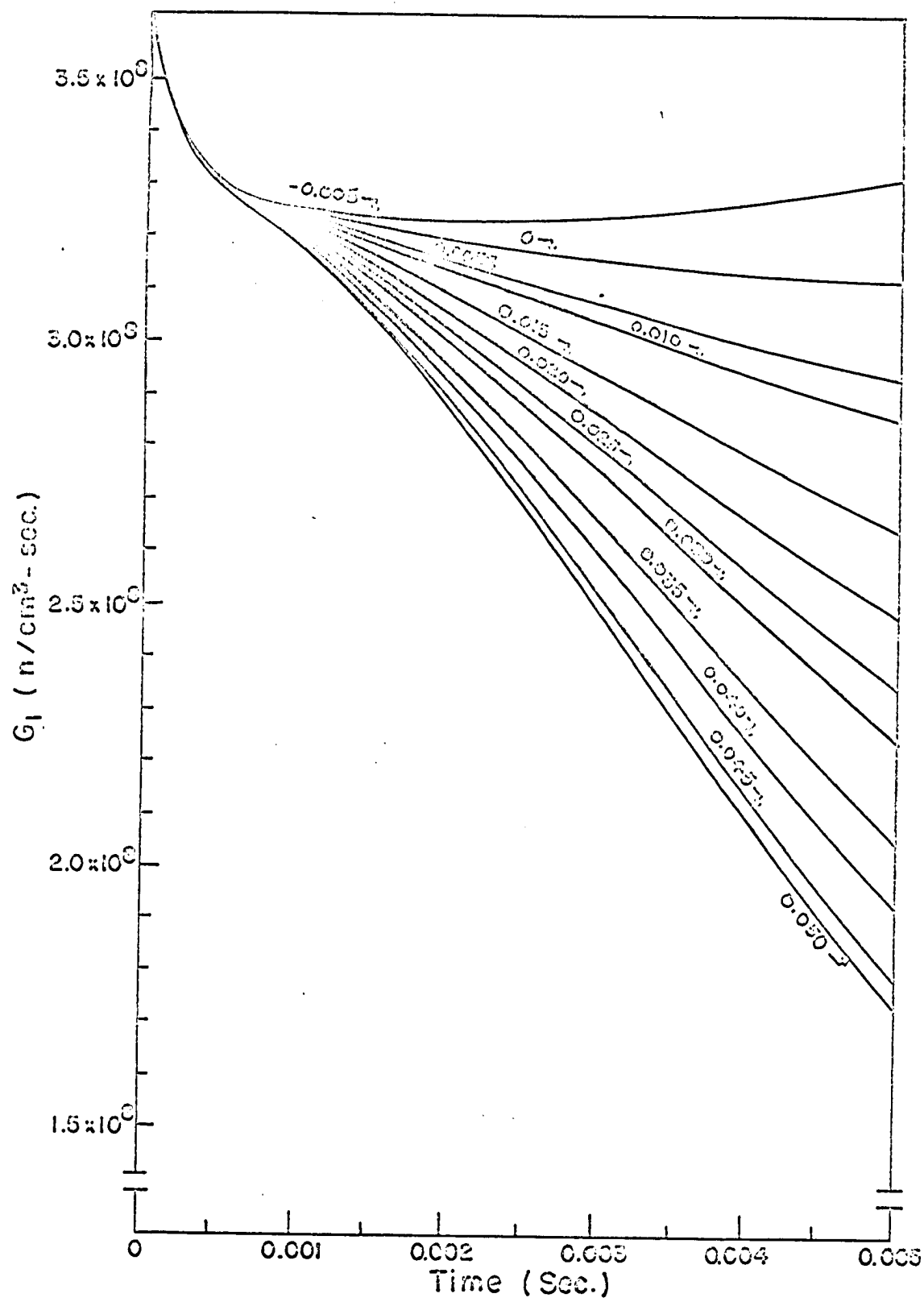


Table 8. Comparison of the analog solutions for the sets of differential equations
 A. Exact differential equations (four roots)

Time (sec)	1B'			1C'			1D'		
	Analog	Theor.	Diff.	Analog	Theor.	Diff.	Analog	Theor.	Diff.
0	3.63	3.63	0.00	3.63	3.63	0.00	3.63	3.63	0.00
0.0010	3.12	3.12	0.00	3.16	3.12	0.04	3.21	3.12	0.09
20	2.86	2.70	0.16	2.89	2.69	0.20	2.97	2.68	0.29
30	2.59	2.35	0.24	2.62	2.32	0.30	2.71	2.32	0.39
40	2.33	2.05	0.28	2.36	2.01	0.35	2.47	2.00	0.47
50	2.10	1.80	0.30	2.13	1.75	0.38	2.27	1.73	0.54
60	1.88	1.59	0.29	1.93	1.52	0.41	2.11	1.49	0.61
70	1.69	1.40	0.29	1.76	1.32	0.44	1.96	1.29	0.67
80	1.54	1.24	0.30	1.63	1.14	0.49	1.83	1.11	0.72
90	1.40	1.10	0.30	1.51	0.99	0.52	1.73	0.96	0.77
100	1.30	0.98	0.32	1.42	0.86	0.56	1.60	0.83	0.77

Table 8. (Continued)

B. Exact differential equations (two roots)

Time (sec)	1B"			1C"			1D"		
	Analog	Theor.	Diff.	Analog	Theor.	Diff.	Analog	Theor.	Diff.
0	3.63	3.63	0.00	3.63	3.63	0.00	3.63	3.63	0.00
0.0010	3.12	3.12	0.00	3.09	3.12	-0.03	3.20	3.12	0.08
20	2.73	2.70	0.03	2.67	2.69	-0.02	2.79	2.68	0.11
30	2.39	2.35	0.04	2.27	2.32	-0.05	2.43	2.32	0.11
40	2.09	2.05	0.04	1.98	2.01	-0.03	2.10	2.00	0.10
50	1.85	1.80	0.05	1.80	1.75	0.05	1.83	1.73	0.10
60	1.63	1.59	0.04	1.49	1.52	-0.03	1.59	1.49	0.10
70	1.44	1.40	0.04	1.29	1.32	-0.03	1.38	1.29	0.09
80	1.26	1.24	0.02	1.13	1.14	-0.01	1.20	1.11	0.09
90	1.13	1.10	0.03	0.97	0.99	-0.02	1.04	0.96	0.08
100	1.01	0.98	0.03	0.86	0.86	0.00	0.92	0.83	0.09

From these results a preliminary conclusion can be deduced: that the proposed simulator contains inherent errors in the amplifiers which add in the synthesis of $G_1(t)$. However, if the number of amplifiers is reduced, (and hence the order of the differential equation being solved), there is not only a marked decrease in the errors but a randomness appears, the errors being sometimes positive, sometimes negative.

In summary, although the analog simulation described in this work is still far from being exhaustively studied, it may be considered, to within accuracies usually accepted for simulator analyses, as adequate for preliminary studies of two-core reactor systems according to the Chezem-Helmick model. There is, however, a tendency toward greater errors in $G_1(t)$ than in $G_2(t)$ because of the addition of individual errors in the amplifiers and there is always a residual error as shown by the curves not being asymptotic to the positive t -axis but to an axis a short distance above it.

CONCLUSIONS AND RECOMMENDATIONS FOR FURTHER STUDY

The analog computer circuit developed in this work for the simulation of the neutronic behavior of the two cores of a coupled-core reactor according to the model of Chezem and Helmick has been checked with the four cases experimentally studied by the proponents of the model, and was found accurate within the accepted limits for analog computer calculations for runs not exceeding about 30 seconds of machine time. It has also been applied to a study of the effect of reactivity drops in either core on the neutron generation rates, and the results obtained have been in accordance with the accepted models of neutron propagation and multiplication processes, except in the case where the effect of reactivity changes in the passive core was considered. In this case however it is suspected that the errors arise from the voltage errors inherent in the amplifiers themselves.

The simulator here proposed is, however, far from being complete. Further research along this line might take two directions: one is to study this simulator for the Chezem-Helmick model in greater detail, using more complex circuits allowing the use of greater number of amplifiers, wider range in voltage and more flexibility in the choice of amplifier gains, preferably to the point where each parameter of the problem enters into the solution by itself and not in combination with others as in the present work. If this can be

done positive and negative errors in the majority of cases will cancel out and the results are expected to be more accurate than those obtained here.

Another direction that this type of research can take is the investigation of the possibility of simulating other models to explain neutronic behavior of coupled-core reactors. Particularly interesting would be a study like this one of the Delta Function Model and the Delayed Shaped Pulse Model, both of which lead to pairs of conjugate complex roots which implies that the solutions would show high frequency oscillations converging to the negative real parts of the roots. The periods of oscillation associated with these complex roots, ranging from 0.08 to 0.30 milliseconds for the delta-function model and about 4 to 5 milliseconds for the delayed shaped pulse model, might give difficulties in time-scaling because the plotter cannot be expected to respond properly to these periods. There is experimental evidence for these small high-frequency oscillations superimposed on the gross response functions, hence provision for these oscillations should be incorporated into the existing theory.

Two other areas of further research can be briefly mentioned: the extension of this method to include temperature effects in both cores, and the simulation of non-linear dynamics models of two-core reactor systems.

LITERATURE CITED

1. Aseltine, John A. Transform method in linear system analysis. New York, New York, McGraw-Hill Book Company, Inc. 1958.
2. Bryant, L. T., Just, L. C. and Pawlicki, G. S. Introduction to electronic analogue computing. United States Atomic Energy Commission Report ANL-6187 [Argonne National Laboratory, Argonne, Illinois]. 1960.
3. Cheng, David K. Analysis of linear systems. Cambridge, Massachusetts, Addison Wesley Publishing Company, Inc. 1959.
4. Chezem, C. G. and Helmick, H. H. Pulsed neutron analysis in the Los Alamos coupled reactor experiment. United States Atomic Energy Commission Report LA-3263-MS [Los Alamos Scientific Laboratory, New Mexico]. 1964.
5. Chezem, C. G. and Seale, R. L. Temperature dependent kinetics of coupled-core reactors. United States Atomic Energy Commission Report LA-3148-MS [Los Alamos Scientific Laboratory, New Mexico]. 1964.
6. Gage, Stephen J. Investigations on the dynamic behavior of coupled-core nuclear reactors. Unpublished Xeroxed Ph.D. thesis, Purdue University, Lafayette, Indiana. Ann Arbor, Michigan, University Microfilms, Inc. 1966.
7. Hang, D. F. and Manning, E. G. Analog computations of training reactor kinetics. Argonne, Illinois, Argonne National Laboratory. 1959.
8. Hansen, G. E. Kinetics equation for a cluster of Rover reactors. Los Alamos Scientific Laboratory Office Memorandum N-2-7967. 1965.
9. Jackson, Albert S. Analog computation. New York, New York, McGraw-Hill Book Company, Inc. 1960.
10. Johnson, Clarence L. Analog computer techniques. New York, New York, McGraw-Hill Book Company, Inc. 1963.
11. Seale, R. L. Coupled core reactors. United States Atomic Energy Commission Report LAMS-2967 [Los Alamos Scientific Laboratory, New Mexico]. 1964.

12. Seale, R. L. Investigation of coupled Rover cores. United States Atomic Energy Commission Report LAMS-2968 [Los Alamos Scientific Laboratory, New Mexico]. 1964.
13. Seale, R. L. and Chezem, C. G. Neutronic behavior of coupled Rover cores. United States Atomic Energy Commission Report LA-CD-6530 [Los Alamos Scientific Laboratory, New Mexico]. 1964.

APPENDIX A

Computation of the K's

$$\beta = 0.0078$$

$$l_1 = l_2 = l = 31 \text{ } \mu\text{sec} = 31 \times 10^{-6} \text{ sec}$$

$$l_1^* = l_2^* = l^* = \frac{l}{\beta} = \frac{31 \times 10^{-6}}{0.0078} = 3.974 \times 10^{-3} \text{ sec}$$

Case I.

$$\epsilon_{12} = \epsilon_{21} = \epsilon = 0.306 \text{ } \$ \text{ (at 6 ft)}$$

$$\tau_{12} = \tau_{21} = \tau = 130 \text{ } \mu\text{sec} = 130 \times 10^{-6} \text{ sec (at 6 ft)}$$

$$\delta k_1^P = -2.200 \text{ } \$$$

$$\delta k_2^P = -2.060 \text{ } \$$$

$$\alpha_1 = \frac{\delta k_1^P}{l^*} = \frac{-2.200}{3.974 \times 10^{-3}} = -553.5$$

$$\alpha_2 = \frac{\delta k_2^P}{l^*} = \frac{-2.060}{3.974 \times 10^{-3}} = -518.3$$

$$\frac{1}{\tau_{12}} = \frac{1}{\tau_{21}} = \frac{1}{\tau} = \frac{1}{130 \times 10^{-6}} = 7,692 \text{ sec}^{-1}$$

$$\begin{aligned} \gamma_{12} = \gamma_{21} = \gamma &= \frac{\epsilon}{l^* \tau} = \frac{0.306}{3.974 \times 10^{-3} \times 130 \times 10^{-6}} = 5.923 \times 10^5 \\ &= 592,300 \end{aligned}$$

$$K_0 = \frac{\gamma}{\tau} = \frac{5.923 \times 10^5}{130 \times 10^{-6}} = 4.556 \times 10^9$$

$$\begin{aligned} K_1 &= \frac{2}{\tau} - \alpha_2 \\ &= \frac{2}{130 \times 10^{-6}} - (-518.3) \end{aligned}$$

$$= 2(7,692) + 518.3 = 15,902 = 1.590 \times 10^4$$

$$\begin{aligned}
 K_2 &= \frac{1}{\tau^2} - \frac{2\alpha_2}{\tau} \\
 &= (7,692)^2 - \frac{2(-518.3)}{130 \times 10^{-6}} \\
 &= 5.917 \times 10^7 + 7.974 \times 10^6 \\
 &= 6.714 \times 10^7
 \end{aligned}$$

$$K_3 = -\frac{\alpha_2}{\tau^2} = -\frac{-518.3}{(130 \times 10^{-6})^2} = 3.067 \times 10^{10}$$

$$\begin{aligned}
 K_4 &= \frac{2}{\tau} - \alpha_1 - \alpha_2 \\
 &= 2(7,692) - (-553.5) - (-518.3) \\
 &= 16,460 \\
 &= 1.646 \times 10^4
 \end{aligned}$$

$$\begin{aligned}
 K_5 &= \frac{1}{\tau^2} - \frac{2(\alpha_1 + \alpha_2)}{\tau} + \alpha_1 \alpha_2 \\
 &= (7,692)^2 - 2(-553.5 - 518.3)(7,692) + (-553.5)(-518.3) \\
 &= 5.917 \times 10^7 + 1.649 \times 10^7 + 2.869 \times 10^5 \\
 &= 7.595 \times 10^7
 \end{aligned}$$

$$\begin{aligned}
 K_6 &= \frac{2\alpha_1 \alpha_2}{\tau} - \frac{\alpha_1 + \alpha_2}{\tau^2} \\
 &= 2(-553.5)(-518.3)(7,692) - (-1071.8)(7,692)^2 \\
 &= 4.414 \times 10^9 + 6.342 \times 10^{10} \\
 &= 6.783 \times 10^{10}
 \end{aligned}$$

$$K_7 = \frac{\alpha_1 \alpha_2}{r^2} - \gamma^2$$

$$= (-553.5)(-518.3)(7,692)^2 - (5.923 \times 10^5)^2$$

$$= 1.698 \times 10^{13} - 3.508 \times 10^{11}$$

$$= 1.663 \times 10^{13}$$

APPENDIX B

Expansion and Evaluation of ΣW_i , $\Sigma R_i W_i$, $\Sigma R_i^2 W_i$, $\Sigma R_i^3 W_i$

$$\begin{aligned} \Sigma W_i &= \frac{1}{(R_1-R_2)(R_1-R_3)(R_1-R_4)} + \frac{1}{(R_2-R_1)(R_2-R_3)(R_2-R_4)} \\ &+ \frac{1}{(R_3-R_1)(R_3-R_2)(R_3-R_4)} + \frac{1}{(R_4-R_1)(R_4-R_2)(R_4-R_3)} \\ &= \frac{[(R_2-R_3)(R_2-R_4)(R_3-R_4) - (R_1-R_3)(R_1-R_4)(R_3-R_4) \\ &\quad + (R_1-R_2)(R_1-R_4)(R_2-R_4) - (R_1-R_2)(R_1-R_3)(R_2-R_3)]}{(R_1-R_2)(R_1-R_3)(R_1-R_4)(R_2-R_3)(R_2-R_4)(R_3-R_4)} \end{aligned}$$

The numerators are of the form

$$\begin{aligned} &(R_a-R_b)(R_a-R_c)(R_b-R_c) \\ &= R_a^2 R_b - R_a R_b^2 + R_b^2 R_c - R_b R_c^2 + R_a R_c^2 - R_a^2 R_c \\ &(R_2^2 R_3 - R_2 R_3^2 + R_3^2 R_4 - R_3 R_4^2 + R_2 R_4^2 - R_2^2 R_4 \\ &- R_1^2 R_3 + R_1 R_3^2 - R_3^2 R_4 + R_3 R_4^2 - R_1 R_4^2 + R_1^2 R_4 \\ &R_1^2 R_2 - R_1 R_2^2 + R_2^2 R_4 - R_2 R_4^2 + R_1 R_4^2 - R_1^2 R_4 \\ &- R_1^2 R_2 + R_1 R_2^2 - R_2^2 R_3 + R_2 R_3^2 - R_1 R_3^2 + R_1^2 R_3) \\ \Sigma W_i &= \frac{\quad}{(R_1-R_2)(R_1-R_3)(R_1-R_4)(R_2-R_3)(R_2-R_4)(R_3-R_4)} = 0 \end{aligned}$$

$$\begin{aligned} & (R_1 R_2^2 R_3 - R_1 R_2 R_3^2 + R_1 R_3^2 R_4 - R_1 R_3 R_4^2 + R_1 R_2 R_4^2 - R_1 R_2^2 R_4 \\ & - R_1^2 R_2 R_3 + R_1 R_2 R_3^2 - R_2 R_3^2 R_4 + R_2 R_3 R_4^2 - R_1 R_2 R_4^2 + R_1^2 R_2 R_4 \\ & + R_1^2 R_2 R_3 - R_1 R_2^2 R_3 + R_2^2 R_3 R_4 - R_2 R_3 R_4^2 + R_1 R_3 R_4^2 - R_1^2 R_3 R_4 \\ & - R_1^2 R_2 R_4 + R_1 R_2^2 R_4 - R_2^2 R_3 R_4 + R_2 R_3^2 R_4 - R_1 R_3^2 R_4 + R_1^2 R_3 R_4) \\ \Sigma R_i W_i &= \frac{}{(R_1 - R_2)(R_1 - R_3)(R_1 - R_4)(R_2 - R_3)(R_2 - R_4)(R_3 - R_4)} = 0 \end{aligned}$$

$$\begin{aligned} & (R_1^2 R_2^2 R_3 - R_1^2 R_2 R_3^2 + R_1^2 R_3^2 R_4 - R_1^2 R_3 R_4^2 + R_1^2 R_2 R_4^2 - R_1^2 R_2^2 R_4 \\ & - R_1^2 R_2^2 R_3 + R_1 R_2^2 R_3^2 - R_2^2 R_3^2 R_4 + R_2^2 R_3 R_4^2 - R_1 R_2^2 R_4^2 + R_1^2 R_2^2 R_4 \\ & R_1^2 R_2 R_3^2 - R_1 R_2^2 R_3^2 + R_2^2 R_3^2 R_4 - R_2 R_3^2 R_4^2 + R_1 R_3^2 R_4^2 - R_1^2 R_3^2 R_4 \\ & - R_1^2 R_2 R_4^2 + R_1 R_2^2 R_4^2 - R_2^2 R_3 R_4^2 + R_2 R_3^2 R_4^2 - R_1 R_3^2 R_4^2 + R_1^2 R_3 R_4^2) \\ \Sigma R_i^2 W_i &= \frac{}{(R_1 - R_2)(R_1 - R_3)(R_1 - R_4)(R_2 - R_3)(R_2 - R_4)(R_3 - R_4)} = 0. \end{aligned}$$

$$\begin{aligned} & (R_1^3 R_2^2 R_3 - R_1^3 R_2 R_3^2 + R_1^3 R_3^2 R_4 - R_1^3 R_3 R_4^2 + R_1^3 R_2 R_4^2 - R_1^3 R_2^2 R_4 \\ & - R_1^2 R_3^2 R_3 + R_1 R_3^2 R_3^2 - R_2^3 R_3^2 R_4 + R_2^3 R_3 R_4^2 - R_1 R_2^3 R_4^2 + R_1^2 R_2^3 R_4 \\ & R_1^2 R_2 R_3^3 - R_1 R_2^2 R_3^3 + R_2^2 R_3^3 R_4 - R_2 R_3^3 R_4^2 + R_1 R_3^3 R_4^2 - R_1^2 R_3^3 R_4 \\ & - R_1^2 R_2 R_4^3 + R_1 R_2^2 R_4^3 - R_2^2 R_3 R_4^3 + R_2 R_3^2 R_4^3 - R_1 R_3^2 R_4^3 + R_1^2 R_3 R_4^3) \\ \Sigma R_i^3 W_i &= \frac{}{(R_1 - R_2)(R_1 - R_3)(R_1 - R_4)(R_2 - R_3)(R_2 - R_4)(R_3 - R_4)}. \end{aligned}$$

Expand the denominator:

$$\begin{aligned} & (R_1 - R_2)(R_1 - R_3)(R_1 - R_4)(R_2 - R_3)(R_2 - R_4)(R_3 - R_4) \\ & = (R_1 - R_2)(R_1 - R_3)(R_2 - R_3)(R_2 - R_4)(R_4 - R_1)(R_4 - R_3) \\ & = (R_1^2 - R_1 R_2 - R_1 R_3 + R_2 R_3)(R_2^2 - R_2 R_3 - R_2 R_4 + R_3 R_4)(R_1 R_3 - R_1 R_4 - R_3 R_4 + R_4^2). \end{aligned}$$

Multiply the second and third factors:

$$\begin{aligned}
 & R_1 R_2^2 R_3 - R_1 R_2^2 R_4 - R_2^2 R_3 R_4 + R_2^2 R_4^2 - R_1 R_2 R_3^2 + R_1 R_2 R_3 R_4 + R_2 R_3^2 R_4 \\
 & - R_2 R_3 R_4^2 - R_1 R_2 R_3 R_4 + R_1 R_2 R_4^2 + R_2 R_3 R_4^2 - R_2 R_4^3 + R_1 R_3^2 R_4 - R_1 R_3 R_4^2 \\
 & - R_3^2 R_4^2 + R_3 R_4^3.
 \end{aligned}$$

Multiply this result by the first factor:

$$\begin{aligned}
 & R_1^3 R_2^2 R_3 - R_1^3 R_2^2 R_4 - R_1^2 R_2^2 R_3 R_4 + R_1^2 R_2^2 R_4^2 - R_1^3 R_2 R_3^2 + R_1^2 R_2 R_3^2 R_4 \\
 & R_1^3 R_2 R_4^2 - R_1^2 R_2 R_4^3 + R_1^3 R_3 R_4^2 - R_1^3 R_3 R_4^2 - R_1^2 R_3^2 R_4^2 + R_1^2 R_3 R_4^3 \\
 & - R_1^2 R_2^3 R_3 + R_1^2 R_2^3 R_4 + R_1 R_2^3 R_3 R_4 - R_1 R_2^3 R_4^2 + R_1^2 R_2^2 R_3^2 - R_1 R_2^2 R_3^2 R_4 \\
 & - R_1^2 R_2^2 R_4^2 + R_1 R_2^2 R_4^3 - R_1^2 R_2 R_3^2 R_4 + R_1^2 R_2 R_3 R_4^2 + R_1 R_2 R_3^2 R_4^2 - R_1 R_2 R_3 R_4^3 \\
 & - R_1^2 R_2^2 R_3^2 + R_1^2 R_2^2 R_3 R_4 + R_1 R_2^2 R_3^2 R_4 - R_1 R_2^2 R_3 R_4^2 + R_1^2 R_2 R_3^3 - R_1 R_2 R_3^3 R_4 \\
 & - R_1^2 R_2 R_3 R_4^2 + R_1 R_2 R_3 R_4^3 - R_1^2 R_3^3 R_4 + R_1^2 R_3^2 R_4^2 + R_1 R_3^3 R_4^2 - R_1 R_3^2 R_4^3 \\
 & R_1 R_2^3 R_3^2 - R_1 R_2^3 R_3 R_4 - R_2^3 R_3^2 R_4 + R_2^3 R_3 R_4^2 - R_1 R_2^2 R_3^3 + R_2^2 R_3^3 R_4 \\
 & R_1 R_2^2 R_3 R_4^2 - R_2^2 R_3 R_4^3 + R_1 R_2 R_3^3 R_4 - R_1 R_2 R_3^2 R_4^2 - R_2 R_3^3 R_4^2 + R_2 R_3^2 R_4^3,
 \end{aligned}$$

which can be reduced to the same form as the numerator; so

$$\Sigma R_1^3 W_1 = 1.$$

APPENDIX C

Sample Computation for the Four-Root Case

$$\alpha_1 = -154.0, \alpha_2 = -308.0, \frac{1}{T} = 7,692, \gamma = 5.923 \times 10^5$$

$$R_1 = \alpha_1 + \frac{\gamma^2}{(\alpha_1 - \alpha_2)(\alpha_1 + \frac{1}{T})^2} = -154.0 + \frac{(5.923 \times 10^5)^2}{(154)(7538)^2} \\ = -154.0 + 40.1 = -113.9$$

$$R_2 = \alpha_2 - \frac{\gamma^2}{(\alpha_1 - \alpha_2)(\alpha_2 + \frac{1}{T})^2} = -308.0 - \frac{(5.923 \times 10^5)^2}{(154)(7384)^2} \\ = -308.0 - 41.8 = -349.8$$

$$R_{3,4} = -\frac{1}{T} \pm \frac{\gamma^2}{(\alpha_1 + \frac{1}{T})(\alpha_2 + \frac{1}{T})} = -7,692 \pm \frac{(5.923 \times 10^5)^2}{(7538)(7384)} \\ = -7692 \pm 79$$

$$R_3 = -7613$$

$$R_4 = -7771$$

$$\Sigma R_i = -1.585 \times 10^4$$

$$\Sigma R_i R_j = 6.633 \times 10^7$$

$$\Sigma R_i R_j R_k = -2.805 \times 10^{10}$$

$$\Pi R_i = 0.236 \times 10^{13}$$

$$s^4 + (1.585 \times 10^4)s^3 + (6.633 \times 10^7)s^2 + (2.805 \times 10^{10})s + 0.236 \times 10^{13}$$

$$U_i = \frac{(R_i - \alpha_2)(R_i + \frac{1}{T})^2}{\prod_j (R_i - R_j)}$$

$$U_1 = \frac{(194.1)(7578)^2}{(235.9)(7499)(7657)} = +0.8229$$

$$U_2 = \frac{(-41.8)(7342)^2}{(-235.9)(7263)(7421)} = +0.1772$$

$$U_3 = \frac{(-7305)(79)^2}{(-7499)(-7263)(158)} = -0.005298$$

$$U_4 = \frac{(-7463)(-79)^2}{(-7657)(-7421)(-158)} = +0.005188$$

$$G_1(t) = 0.8229e^{-113.9t} + 0.1772e^{-349.8t} - 0.005298e^{-7613t} \\ + 0.005188e^{-7771t}$$

$$V_i = \frac{\gamma(R_i + \frac{1}{T})}{\prod_j (R_i - R_j)}$$

$$V_1 = \frac{(5.923 \times 10^5)(7578)}{(235.9)(7499)(7657)} = +0.3313$$

$$V_2 = \frac{(5.923 \times 10^5)(7342)}{(-235.9)(7263)(7421)} = -0.3420$$

$$V_3 = \frac{(5.923 \times 10^5)(79)}{(-7499)(-7263)(158)} = +0.005437$$

$$V_4 = \frac{(5.923 \times 10^5)(-79)}{(-7657)(-7421)(-158)} = +0.005212$$

$$G_2(t) = 0.3313e^{-113.9t} - 0.3420e^{-349.8t} + 0.005437e^{-7613t} \\ + 0.005212e^{-7771t}$$

$$\sum U_i (R_j + R_k + R_l) = 1.569 \times 10^4$$

$$\sum U_i \sum R_j R_k = 6.390 \times 10^7$$

$$\Sigma U_i \Sigma R_j R_k R_l = 1.822 \times 10^{10}$$

$$s^3 + (1.569 \times 10^4) s^2 + (6.390 \times 10^7) s + (1.822 \times 10^{10})$$

APPENDIX D

Sample Computation for the Two-Root Case

From Appendix C

$$R_1 = -113.9 \qquad U_1 = 0.8229 \qquad V_1 = 0.3313$$

$$R_2 = -349.8 \qquad U_2 = 0.1772 \qquad V_2 = -0.3420$$

$$M_1 = U_1 + U_2 = 0.8229 + 0.1772 = 1.0001$$

$$\begin{aligned} M_2 &= -U_1 R_2 - U_2 R_1 = -(0.8229)(-349.8) - (0.1772)(-113.9) \\ &= 287.9 + 20.2 = 308.0 \end{aligned}$$

$$M_3 = V_1 + V_2 = 0.3313 - 0.3420 = -0.0107$$

$$\begin{aligned} M_4 &= -V_1 R_2 - V_2 R_1 = -(0.3313)(-349.8) - (-0.3420)(-113.9) \\ &= 115.9 - 39.0 = 76.9 \end{aligned}$$

$$M_5 = -R_1 - R_2 = -(-113.9) - (-349.8) = 463.7$$

$$M_6 = R_1 R_2 = (-113.9)(-349.8) = 3.984 \times 10^4$$

$$\frac{g_1(s)}{A} = \frac{s + 308}{s^2 + 463.7s + 3.984 \times 10^4}$$

Let $s = 10^3 s_m$.

$$\begin{aligned} \frac{g_{1m}(s)}{A_m} &= \frac{10^3 s_m + 308}{10^6 s_m^2 + 463.7 \times 10^3 s_m + 3.984 \times 10^4} \\ &= \frac{10^3 (s_m + 0.308)}{10^6 (s_m^2 + 0.4637 s_m + 0.03984)} \end{aligned}$$

$$\text{or } \frac{g_{1m}(s)}{m} = \frac{s_m + 0.308}{s_m^2 + 0.4637 s_m + 0.03984}$$